Obstructive Sleep Apnea Syndrome Monitoring and CPAP Recovery.

Submitted by:

Mohammed A.H. Qaymari

Supervisor:

Dr. Ramzi Alqawasmi

Submitted to the College of Engineering

in partial fulfillment of the requirements for the degree of

Bachelor degree in Biomedical Engineering

Palestine Polytechnic University

Jan 2021

الإهداء

إلى معلمنا وقائدنا وقدوتنا وحبيبنا وشفيعنا محمد صلى لله عليه وسلم.
إلى من رسموا بدمائهم خارطة الوطن وطريق المستقبل وهندسوا بأجسادهم معاقل العزة والكرامة إلى من هم أكرم منا جميعا إلى شهداء الوطن الحبيب.
إلى الذين عشقوا الحرية التي تفوح منها رائحة الياسمين وتوارو خلف القضبان ليفسحوا لنا النور إلى أسر انا الأبطال.
إلى التي رآنا قلبها قبل عينيها واحتضنتنا أحشائها قبل يديها إلى التي تعجز الكلمات عن شكرها إلى منبع الحنان وتاج الرأس ومن تنحني لها جباهنا، كيف لا والجنة تحت إقدامها، أمهاتنا الفضيلات.
إلى من وصلو النهار بالليل، و بذلو الغالي و النفيس من أجلنا، إلى مصدر فخرنا و عزنا، آبائنا الكرام.
إلى من يحملون في قلوبهم ذكرياتنا ويتقاسمون معنا أفراحنا وهمومنا ومن ساندونا، إخوتنا وأخو اتنا الأعزاء.
إلى من ضاقت السطور لذكرهم فوسعتهم قلوبنا، أصدقائنا الأعزاء.
إلى من علمونا حروفا من ذهب وكلمات من درر، إلى من جعلو أفكارهم منارة تنير لنا الطريق، إلى محبي العلم والمعرفة، أساتذتنا الاكارم.
إلى من رسم معنا خطوات هذا النجاح، إلى من بذل جهده ووقته وكان لنا مرشدا وناصحا وأخا إلى المشرف الحبيب الدكتور رمزي القواسمة.
إلى صرحنا العظيم ومكمن فخرنا وصانعه مجدنا إلى بيتنا الثاني التي قضينا فيها أجمل أيامنا جامعتنا الحبيبة.
إلى محفزنا الأول والأخير إلى قبلتنا ومقصد بوصلتنا إلى من احتضنتنا كل هذه السنين رغم أوجاعها إلى دولتنا الفلسطينية وجوهرتها القدس الشريف.
إلى الزملاء وكوادر جامعه بوليتكنك فلسطين.

محمد القيمري

Acknowledgments

I expresses my thanks to all who made this project a reality. Special thanks to the biomedical engineering staff, including:

Eng. Ali Amro, Dr. Abdullah Arman,
Eng Fidaa Ja'afra, Eng. Firas Alhaddad, Eng. Arfat Zalloum, and especially to Dr. Ramzi Qawasmeh , my graduating project supervisor for his support and encouragement.

Always, I have had enormous support and encouragement from my family and friends and our gratitude for their patience can never be fully expressed.

Mohammed Alqaimari

Abstract

Obstructive sleep apnea (OSA) is a highly prevalent disease characterized by recurrent episodes of upper airway obstruction that result in recurrent arousals and episodic oxyhemoglobin desaturations during sleep. When the obstructive sleep apnea happens to the patient, the air cannot flow normally into the lung and may cause to stop the breathing for short periods of time. The block in airflow is usually caused by the collapsed of soft tissues in the tongue and in the back on the throat (upper airflow). These pauses in airflow can occur off and on during sleep that can causes many serious problems if not treated probably.

Several research demonstrate that patients with obstructive sleep apnea have complex metabolic abnormalities and manifest with a time, like high blood pressure, periods of stopping breathing especially in the sleeping, heart disease, stroke or early death. There are many clues and symptoms that can be noticed on the patient, and can be as an introduction for obstructive sleep apnea like a Loud snoring , Excessive daytime sleepiness, Observed episodes of stopped breathing during sleep, Abrupt awakenings accompanied by gasping or choking, High blood pressure, Nighttime sweating. By monitoring some of important physiological parameters of the patient, like a heart rate, airflow and the movement of the patient’s chest, obstructive sleep apnea syndrome can be early detected and treated.

The idea of this project is to design a device that has the ability to deal with obstructive sleep apnea syndrome cases. Obstructive sleep apnea is a common problem that effects on the breathing’s of the patient during a sleep. Two parameters (Respiratory rate and the movement of the chest) can be measure using a device that compare it with a reference values in the arduino, and if the reading of parameters are abnormal, the device will active a buzzer with a red light to be signs of emergency case, and then activate an efficient recovery system like CPAP that can deal with the case, at the same time, the Arduino microcontroller will send the data via Bluetooth to the doctor of the patient or any related person.

المُلَخَّصْ

يُشَكِّل انقطاع النفس الانسدادي النومي اضطرابًا خطيرًا يَحدُث أثناء النوم. إذ يُؤدِّي إلى انقطاع النَّفَس بشكل متكرِّر، ويبدأ أثناء النوم. رغم وجود عدة أنواع من انقطاع النفس النومي، فإن أكثرها شيوعًا هو انقطاع النفس الانسدادي النومي. يَحدُث هذا النوع من انقطاع النفس عندما تسترخي عضلات الحلق بشكل متقطِّع وتُغْلِق مجرى الهواء أثناء النوم. ويُعَدُّ الشَّخير من العلامات الملحوظة على انقطاع النفس الانسدادي النومي. يمكن أن يؤدي الحرمان المزمن من النوم بسبب انقطاع النفس أثناء النوم إلى النعاس أثناء النهار ، وضعف التركيز ، وزيادة مخاطر الحوادث خاصة فى حالة قيادة السيارة. يمكن أن يؤدي أيضًا على المدى البعيد إلى مشاكل صحية جسدية أخرى خطيرة مثل السكر وأمراض القلب ومشاكل الكبد وزيادة الوزن.

عندما يشعر المريض بالاعراض المرضية التي تم ذكرها سابقا فإنه يقوم باستخدام الجهاز للتأكد من حالته الصحية، حيث يقوم الجهاز بقياس معدل التنفس و معدل نبضات القلب وعدد حركات الصدر. بعد ذلك يقوم الجهاز بعرض القراءات التي حصل عليها من المجسات على شاشة مرفقة (LCD)،ومن ثم يعمل على مقارنة القيم التي حصل عليها مع قيم مرجعية مخزنة داخل (Arduino) ، فاذا تجاوزت القيم التي حصل عليها عن القيم المخزنة فان الجهاز يطلق انذاراً وضوء أحمر وهو عبارة عن مؤشر لدخول المريض في متلازمة انسداد النوم التنفسي ، ليقوم بعدها الجهاز بتفعيل طريقة علاجية لمساعدة المريض على فتح الانسداد ومن ثم أخد العلاج المناسب.

تقوم الفكرة الرئيسية للمشروع على تصميم جهاز لدية القدرة على التعامل والتنبؤ المبكر بمتلازمة انسداد النوم التنفسي ، ويعتمد التنبؤ المبكر بهذه المتلازمة على استخدام مجموعة من الحساسات التي تستخدم لقياس مقدار التغير الموجود في جسم الانسان لمجموعة من العلامات الفسيولوجية . حيث أنه تم استخدام سنسور حرارة لحساب معدل التنفس من خلال وضعه على قناع يثبت على فم المريض ومراقبة حركة صدر المريض كحساس مساعد لمعرفة وضع التنفس لدى المريض ، سيتم معالجة هذه الإشارات من خلال متحكم الأردوينو أونو، الذي يعمل على مقارنة هذه النتائج مع قيم مرجعية مخزنة بداخلة، وبناء على هذخ النتائج، سيقوم المتحكم بعرض النتائج على شاشة صغيرة وارسال النتائج لهاتف الطبيب المختص أو لشخص ذو علاقة.

Table of Contents

Chapter One: - Thesis Overview

Chapter Two: - Diabetes Pathophysiology

Chapter Three: - Technology Background

Chapter Four: - System Design

Chapter Five: - System Implementation

Chapter Six: - Results and conclusions

List of Figures

List of Tables

List of Abbreviation

Abbreviation	**Full Meaning**
OSA	Obstructive sleep apnea
HR	Heart Rate
PPM	Part Per Million
BPM	Beat Per Minute
IR	Infra Red
Op-Amp	Operational Amplifier
ADC	Analog to Digital Converter
DAC	Digital to Analog Converter
LED	Light Emitted Diode

Chapter One
Thesis Overview

Chapter One

Thesis Overview

Obstructive sleep apnea syndrome is a clinical disorder marked by frequent pauses in breathing during sleep usually accompanied by loud snoring. These pauses cut off the oxygen supply to your body for a few seconds and halt the removal of carbon dioxide. As a result of this, your brain briefly wakes you up, re-opens the airways and re-starts breathing. This can occur many times during the night and makes proper sleep impossible. Other reported outcomes of sleep apnea include respiratory failure, hypertension, heart attack, neuropsychological dysfunction, stroke and heart disease.

Obstructive sleep apnea syndrome is diagnosed through polysomnography, a method of recording body activity during sleep; and pulse oximetry, which measures the amount of oxygen in the blood at any time. Obstructive sleep apnea syndrome is not a life-threatening condition in itself, but it can result in serious problems such as cardiovascular and cerebrovascular diseases. The disease can impact on the quality of life, but can be easily managed. One of the treatments is continuous positive airway pressure, which forces air through a mask into the airways so that they do not close.

1.1 Project Idea Description

In this project a portable obstructive sleep apnea syndrome monitoring and CPAP recovery will be designed and implemented, this device will read the number of respiratory rate and the motion of the patient chest, and then send these data to the microcontroller system, this microcontroller is processed the data and then display the processed data on the LCD or using Bluetooth to send the data to application that installed on the doctor phone or any related person, the system is connected with alarm system that will be activated when the data excess the threshold amount memorized in the system, which enable the device to treat with the case by running a therapeutic device.

1.2 Project Motivation

Most people didn't notice if they are suffered from obstructive sleep apnea and treat with this syndrome. Early detection and treatment are the keys to avoid serious symptoms that may cause a problem in cardiovascular and respiratory system within days if didn't treated early.

A reliable, noninvasive diagnostic method will be invented to impose less physical and financial burden on patients who suffer from obstructive sleep apnea syndrome, and protect the patient from the obstructive sleep apnea side effects.

1.3 Project Aims

The main objectives of this project can be summarized as follow:

- Help patients with obstructive sleep apnea to improve daily functioning.
- Help patients with obstructive sleep apnea to know the number of heart rate and respiratory rate.
- Eliminate respiratory disturbances and Reduce daytime sleepiness.
- Help seniors and young who face this problem to reducing the risk of stroke.
- The good treatment of the case of obstructive sleep apnea decreased traffic and other work-related accidents in addition to enhancing work productivity.

1.4 Literature Review and Related Work

The Obstructive Sleep Apnea-Hypopnea Syndrome features as a disorder caused by repetitive and intermittent closing of the upper airways during sleep, due to the collapse of the pharynx wall [1]. The hypopnea and apnea are distinct terms; the first one refers to a transitory and incomplete reduction, of least 50% of the air flow to lungs and the second one, the absence of breathing [2] , lasting less than 10 seconds [3]

The obstruction of the air flow is frequently followed by the reduction of the oxy-hemoglobin saturation, which has as mainly symptoms the loud snoring, apnea periods, fragmented sleep and frequent awakenings causing daytime sleepiness [4].The clinical characteristics of OSAHS are classified as daytime and nighttime. Excessive sleepiness, hypossalivation, gastroesophageal reflux, sexual incapacity, irritability, depression, lack of concentration and headaches are classified as daytime manifestations [1,5]. The nighttime are breathing interruptions during sleep, restless sleep, breathe heavily, and diaphoresis [6].

The early diagnose of OSAHS provides the establishment of an efficient treatment according to the disease severity, age and systemic conditions of the patient. Although this syndrome had been known for decades and there are innumerous studies, it is estimated that 93% of women and 82% of men with moderated or severe OSAHS are not diagnosed [7,8].

The Dentist Surgeon can be the first professional to recognize this syndrome in the patient. When sedated, many patients carrying OSAHS present gastroesophageal reflux, due to the effort provoked by the upper airways obstruction, increasing therefore the risk of accidental aspiration and consequently lungs damage, being the reflux uncomfortable, similar to the chest pain reported in dental office [1].

The healthcare professionals should always evaluate the patient in a multidisciplinary manner, analyzing morphologic characteristics as craniofacial alterations may predispose the patient to OSAHS. Researches reveal that when this syndrome is early diagnosed, there are improvements significantly gained on treatment[9].The methods of diagnose vary, being developed in subjective and/or objective way. According to the authors Patil et al. (2010) [10], subjective instruments are much more used in populations studies to the identification of subjects with higher chance in developing the disease, such as the Berlin questionnaire. Also, it is investigated the clinical aspects presented in patient, for instance: fatigue, daytime hypersleepiness, often related to traffic or work accidents due to the difficultness to pay attention, irritability, lack of libido and sexual incapacity, besides morning headaches[11].

In physical evaluation, the anthropometric variables (weigh and high) are assessed, the neck circumference and blood pressure. It is stressed as higher predictive value the neck circumference, body mass index and the presence of arterial hypertension, since this pathology is associated to OSAHS [12].The overnight acidimetry is the register of the pulse acidimetry, developed with or without supervision. However, it presents low specificity, not being much recommended to diagnose the OSAHS [12]. Muller's maneuver is another way to diagnose and, consists on the evaluation of the collapse of the nasal and/or hypopharyx, according to the reduction of the cross section area of the airway .

Through the cephalometric evaluation, the speech therapist can diagnose orofacial myofunctional disorders, among them, the oral breathing, speech disorders of musculoskeletal cause, temporomandibular disorders and the obstructive sleep apnea[13]. In some cases, the cephalometry is only a complementary method. The polyssonography (PSG) is the gold pattern method to diagnose the OSAHS, even if is clinically evident, only can be confirmed by PSG .

The polyssonography is a quantitative and specific exam, which consists in continuous monitoring the physiologic variables, such as electroencephalogram, eye movements, thoracoabdominal, airflow and the tone of the submental muscles, aiming to characterize the quantity and quality of sleep [11].

1.5 Economical Study

This section lists the overall cost of the project components that are considered in implementing this system.

Table (1.1) contains the main required hardware components of the project design, and its estimated cost.

Table (1.1): Estimated Component Cost.

Type	Price	Quantity
1- Arduino Mega & Uno	40 JD	1
2- Flexi-Force sensor	20 JD	1
3- Heart rate sensor	40 JD	1
4- Amplifiers, transistors	20 JD	4
5- Resistors, capacitors, ,wires ,solders	10 JD	(10,4,20)
6- Battery	20 JD	1
7- CPAP device	700 JD	
	Total Price = 850 JD	

1.7 Schedule Time

In this section we make a plan for the predictive project tasks due to the time zone of both coming semesters, this time plan shown in the table (1.3) and table (1.4).

Table (1.2): Timing Schedule of the Summer Semester.

Task/Week	1	2	3	4	5	6	7	8
Collect Information								
Basic Design								
Specification Design								
Documentation								
Advance feature								

Table (1.3): Timing Schedule of the First Semester.

Task/Week	1	2	3	4	5	6	7	8	9	10	11	12	13	14	15
Full Designing															
Purchasing the components															
System implementation															
System analysis															
Documentation															

Chapter Two
Obstructive Sleep Apnea

Chapter Two

Obstructive Sleep Apnea (OSA)

Obstructive sleep apnea is a relatively new condition that is beginning to gain the attention of health care professionals. This disorder has been implicated to affect up to 20% of the population and is characterized by repeated apneic episodes during sleep, which are terminated by brief arousals from sleep. These events prevent the patient from attaining the deeper stages of sleep, which are physiologically needed. The hallmarks of this disorder include snoring and excessive daytime sleepiness. Additionally, OSA may cause daytime systemic hypertension, myocardial ischemia, and other cardiovascular disorders. Currently, the preferred method of conservative treatment for OSA is continuous positive airway pressure. The outcomes for this intervention is still not well understood, as this is a relatively newly identified area of medicine.

2.1 EPIDEMIOLOGY OF OSA

The prevalence of OSA in the general population is still unclear. Several epidemiological studies have attempted to examine this issue. Epidemiological data from Young, Palta, Dempsey, et. al (1993) estimated that in a group of 602 middle aged individuals 2% of women and 4% of men meet the minimal diagnostic criteria for sleep apnea, which is an AHI > 5 and 3 symptoms of daytime hypersomnolence. Excessive daytime sleepiness, an unrefreshed feeling after awakening, and uncontrollable daytime sleepiness which interferes with daily living, were the 3 symptoms of daytime hypersomnolence used in this study. In a more recent epidemiological study by Martin, Gascon, Carrizo, et. al (1997) the prevalence of OSA in southern Europe was examined. A total of 1222 subjects (597 males, 625 females) participated in this study. This diagnosis of OSA was established utilizing three criteria. The first criterion was loud (severe) snoring. Severe snoring was assessed, through a sleep questionnaire, by an interviewer at each subject’s home. The second criterion of excessive daytime sleepiness was also assessed through this interview. The final criterion for diagnosing OSA was an abnormal, nocturnal home oximetry in the presence of repetitive short duration SaO2 fluctuations. The diagnosis of OSA was established in 18 subjects (13 males, 5 females).

2.2 PATHOPHYSIOLOGY

Patency of the upper airway is necessary for respiration to function normally. The feature of a collapsible airway is what creates the potential for upper airway narrowing and possible closure. During swallowing, speech, or regurgitation, upper airway narrowing or closure is needed for these actions to occur. In patients with OSA the collapse of the upper airway during sleep leads to apneic or hypopneic episodes. The result of this disruption in airflow includes a decrease in the SaO2, an increase in blood pressure, increased PaCO2 and metabolic alkalosis. The respiratory disturbance is usually terminated by a brief brain arousal from sleep and breathing is restored as the muscles of the upper airway increase their tone.

The specific site of upper airway occlusion varies among OSA patients. The 3 primary sites that are commonly implicated include the oropharynx, hypopharynx, and nasopharynx. The nasopharynx extends form the end of the nasal septum to the margin of the soft palate. The oropharynx begins at the margin of the soft palate and ends at the tip of the epiglottis. Finally, the region of the hypopharynx is from the tip of the epiglottis to the vocal cords (Isoni, Feroah, Hajduk, et. al (1993). There are many muscles which contribute to maintaining patency of the upper airway. A few of these muscles include the levator and tensor veli palatini, palotoglossus, stylopharyngeus, genioglossus, and hypoglossus. While awake the muscles of the upper airway exert high levels of tonic activity during inspiration to maintain an open airway. During sleep there is a considerable loss of tonic activity in the muscles of the upper airway which predisposes to upper airway collapse (Hudgel (1992). The normal process of ventilation is a key to understanding the mechanisms responsible for OSA. Ventilation is dependent upon air flowing down a gradient of pressure. The inspiratory muscles, with the diaphragm being the largest contributor to inspiration, generate a negative intrapleural pressure that is transmitted to the airway. The ability of the upper airway to maintain its rigidity and stay open is dependent upon the dilator muscles to counteract the negative inspiratory pressure being generated to take air into the lungs. Therefore, the degree of obstruction in the upper airway is a balance between the collapsing forces and the dilating forces. As stated previously, there is a loss of tonic activity in the upper airway muscles during sleep and these muscles cannot maintain a patent airway against the negative inspiratory pressure. The synchronization between these forces is very important. The upper airway muscles must begin contracting and generate greater forces than the inspiratory muscles during inspiration. Under normal conditions this occurs and sleep is uninterrupted as the upper airway is stabilized. In OSA the inspiratory pressure is greater than the stabilizing forces of the upper airway and a degree of obstruction occurs (Kuna and Sant'Ambrogio (1991) and Dempsey and Skatrud (1986).

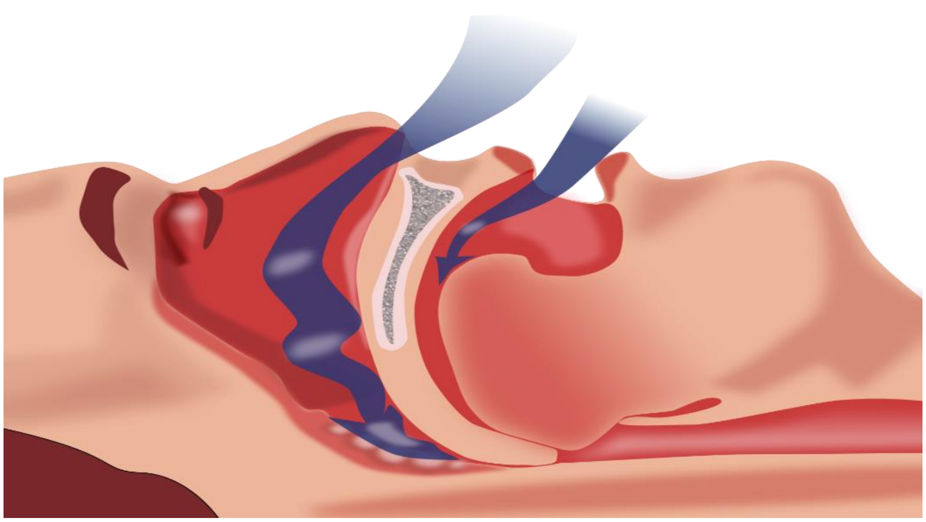

Figure (1): Obstructive sleep apnea.

2.3 Respiration Physiology

Movement of inspired gas into and exhaled gas out of lung is called as ventilation. Understanding of lung volumes, lung compliance, ventilation-perfusion and bronchomotor tone are essential for clinical application of respiratory physiology in anaesthesia and critical care.

2.3.1 Lung volumes

Normal requirements of the body can be easily met by normal tidal ventilation which is approximately 4–8 ml/kg. Body has kept mechanism to provide extra ventilation in the form of inspiratory reserve volume and expiratory reserve volume whenever required (e.g., exercise). When an individual, after tidal expiration, takes full inspiratory breath followed by expiration to reserve volume, it is called as vital capacity breath and is 4–5 L in an average 70 kg individual. There is always some amount of air remaining in the alveoli which prevents it from collapsing. The volume remaining in the lungs after vital capacity breath is called as residual volume.

Residual volume with expiratory reserve volume is called as functional residual capacity (FRC). FRC is basically the amount of air in the lungs after a normal expiration. Gases remaining in the lungs at the end of expiration not only prevent alveolar collapse but also it continues to oxygenate the pulmonary blood flowing though the capillaries during this time period. Reported FRC values vary with various reports but on average it is between 2.8 and 3.1 L in standing position. FRC varies with change of position, anesthesia and body weight. FRC is the reserve which prolongs non-hypoxic apnea time. The portion of the minute ventilation which reaches alveoli and takes part in the gas exchange is called as alveolar ventilation. Normal value of alveolar ventilation is approximately 5 L/min which is similar to the volume of blood flowing through the lung (cardiac output 5 L/min). This makes alveolar ventilation to perfusion ratio approximately one.

2.3.2 RESPIRATORY MECHANICS

Lungs are like inflatable balloon which distend actively by positive pressure inside and/or negative pressure created in pleural space. In normal respiration, negative pleural pressure (Ppl) is sufficient to distend the lungs during inspiratory phase. Understanding of distending pressure is very important to understand the respiratory mechanics. Distending pressure can be known as transpulmonary pressure (Ptp).

2.3.3 Compliance and ventilation of lung

Compliance is expressed as the distension of lung for a given level of Ptp. It is usually 0.2–0.3 L/cm H_2O, Compliance (ability of lung to distend) depends upon the volume of the lung. Compliance is lowest at extremes of FRC. It implies that expanded lung and completely deflated lung has lower capacity to distend to a given pressure as shown in Figure 2. In the upright lung, intra-Ppl varies from the top to the base of the lungs. Intra-Ppl becomes 0.2 cm H_2O positive for every centimetre distance from apex to base of lung. Average height of lung is about 35 cm. In quite breathing, the intra-Ppl at apex is about − 8 cm of H_2O while at base it is − 1.5 cm of H_2O. This means that the alveoli at the apex are exposed to a greater distending pressure ($PA-Ppl = 0 - (-8) = 8$ cm H_2O) compared to those at the base ($PA-Ppl = 0 - (-1.5) = 1.5$ cm H_2O). As already distended, apical region becomes less compliant than other area of lung. This explains the preferential distribution of ventilation to the alveoli at the base of the lungs in upright posture. Distribution of ventilation changes with the position of individual because of the change of Ppl with the gravity.

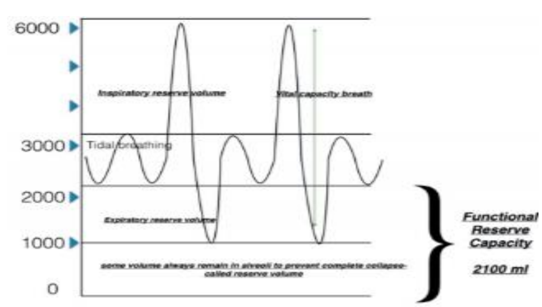

Figure 2: Lung Volume.

2.3.4 Respiratory Muscles

The respiratory muscles are morphologically and functionally skeletal muscles. The group of inspiratory muscles includes the diaphragm, external intercostal, parasternal, sternomastoid, and scalene muscles. The group of expiratory muscles includes the internal intercostal, rectus abdominis, external and internal oblique, and transverse abdominis muscles. During low breathing effort (i.e., at rest) only the inspiratory muscles are active. During high breathing effort (i.e., exercise) the expiratory muscles become active as well.

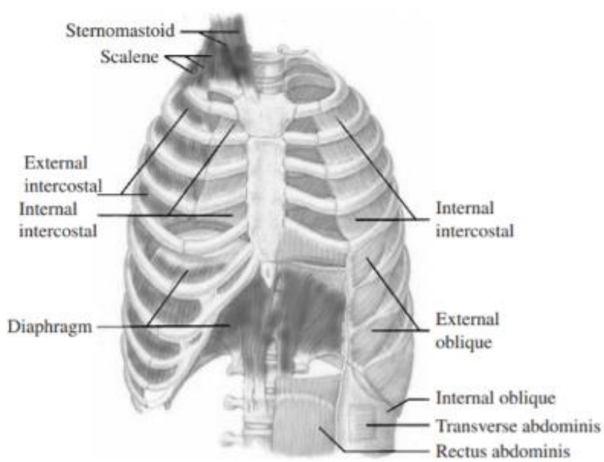

Figure 3 : the anatomy of human respiratory muscles

The diaphragm, the main muscle of inspiration, is a thin, flat, musculotendinous structure separating the thoracic cavity from the abdominal wall. The muscle fibers of the diaphragm radiate from the central tendon to either the three lumbar vertebral bodies (i.e., crural diaphragm) or the inner surfaces of the lower six ribs (i.e., costal diaphragm) as shown in Figure . The tension within the diaphragmatic muscle fibers during contraction generates a caudal force on the central tendon that descends in order to expand the thoracic cavity along its craniocaudal axis. In addition, the costal diaphragm fibers apply a force on the lower six ribs which lifts and rotates them outward.

2.3.5 Mechanics of Breathing

Inhalation is initiated by the contraction of the diaphragm which contracts and descends about 1 cm during normal breathing and up to 10 cm on forced breathing. The diaphragm lines the lower part of the thorax, sealing it off air-tight from the abdominal cavity below. Its contraction causes muscles in the thorax to pull the anterior end of each rib up and outwards enlarging its volume. As a result, the pressure inside the thorax (intrathoracic pressure) and inside the lungs (intrapulmonary pressure) decreases relative to the outside atmospheric air pressure. The pressure difference induces the inhaled air from a higher pressure to a lower pressure in order to equalize the pressure. During exhalation the lung and chest wall return to its equilibrium position and shape. The thoracic cavity volume is reduced and the pressure builds up to release the air from the lungs. In quiet breathing only the elastic recoil of the lung and chest walls is needed to return the thorax to equilibrium (a passive process). However in forceful expiration additional muscles (inter costal) in the thorax and abdomen are also used to further increase the pressure.

2.4 Sleep Apnea for Adult

Sleep apnea is a potentially serious sleep disorder that occurs when a person's breathing is interrupted during sleep. People with untreated sleep apnea stop breathing repeatedly during their sleep, sometimes hundreds of times during the night.

There are two types of sleep apnea: obstructive and central. Obstructive sleep apnea (OSA) is the more common of the two. Obstructive sleep apnea is characterized by repetitive episodes of complete or partial upper airway blockage during sleep. During an apnea episode, the diaphragm and chest muscles work harder as the pressure increases to open the airway. Breathing usually resumes with a loud gasp or body jerk. These episodes can interfere with sound sleep, reduce the flow of oxygen to vital organs, and cause heart rhythm irregularities.

In central sleep apnea (CSA), the airway is not blocked but the brain fails to signal the muscles to breathe due to instability in the respiratory control center. Central apnea is named as such because it is related to the function of the central nervous system.

2.4.1 RISK FACTORS of OSA

Several risk factors may predispose an individual to OSA. The risk factors, which have been most frequently examined, include obesity, snoring,allergic rhinitis. Several studies have reported the association between obesity and OSA. Rossner, Lagerstrand, Persson, et. al (1991) followed 34 obese men referred to an Obesity Unit for 13 a period of 4 years. Of the 22 men who underwent a PSG, 15 (68%) were noted to have significant OSA (mean AI=46). Nine men never attended the PSG study; 3 of who had already died. In the other 3 cases, the recordings did not allow any conclusions to be drawn. The prevalence of OSA in obese females has also been documented by Richman, Elliott, Burns, et. al (1993). In their study 33 of 86 eligible women (BMI>30kg/m 2 and age>18 yr) volunteered to undergo a PSG. Of the 33 PSG's, 29 had successful recordings. The prevalence of OSA (RDI > 5) was 37.9%. Additionally, there was a significant, positive correlation between RDI and BMI in the group which underwent the PSG.

Snoring is another risk factor that has been examined in association with OSA. In the past, snoring was viewed as a mere annoyance. Only recently have the severe implications of snoring been realized. In one study, a total of 35 patients with a history of loud snoring were examined for OSA. Each patient underwent a sleep study to diagnose OSA. It was found that 16 (46%) of the 35 participants demonstrated OSA (Woodhead, Davies, and Allen (1991).

2.4.2 OSA Symptoms

Often the first signs of OSA are recognized not by the patient, but by the bed partner. Many of those affected have no sleep complaints. The most common symptoms of OSA include:

- Snoring.
- Daytime sleepiness or fatigue.
- Restlessness during sleep.
- Sudden awakenings with a sensation of gasping or choking.
- Dry mouth or sore throat upon awakening.
- Intellectual impairment, such as trouble concentrating, forgetfulness, or irritability
- Night sweats.
- Sexual dysfunction.
- Headaches.

People with CSA more often report recurrent awakenings or insomnia, although they may also experience a choking or gasping sensation with sudden awakenings.

2.4.3 Apnea Spells

An apneic spell is usually defined as a cessation of breathing for 20 seconds or longer or a shorter pause accompanied by bradycardia (<100 beats per minute), cyanosis, or pallor. In practice, many apneic events in preterm adult are shorter than 20 seconds, because briefer pauses in airflow may result in bradycardia or hypoxemia. On the basis of respiratory effort and airflow, apnea may be classified as central (cessation of breathing effort), obstructive (airflow obstruction usually at the pharyngeal level), or mixed. The majority of apneic episodes in preterm infants are mixed events, in which obstructed airflow results in a central apneic pause, or vice versa.

Some factors contributing to apnea is a respiratory distress like an airway obstruction, cardiovascular disorders like a congestive heart failure, gastrointestinal disorders like a vomiting, central nervous system disorders incompletely growth and etc.

Cessation of respiratory effort with cyanosis, pallor, hypotonia, or bradycardia is noted. Frequent swallowing-like movements in the pharynx during apnea can be a problem, because swallowing directly inhibits the respiratory drive.

2.4.4 TREATMENT OF OBSTRUCTIVE SLEEP APNEA

The treatment of obese patients with moderate OSA must initially start with some of the lifestyle changes. Some of these modifications include exercise, weight loss, [14-15] decreased alcohol consumption, smoking cessation, altered sleeping position, and nasal continuous positive airway pressure [16-17]. There are certain medications which should be avoided as those drugs may worsen OSA such as alcohol which reduces the tone of the genioglossus and increases collapsibility of upper airway. Then, there is opioids which decrease the rate and depth of respiration, induce chest and abdominal wall rigidity, reduce upper airway patency and blunt respiratory response to carbon dioxide and hypoxia. Also, other central nervous system depressants like benzodiazepines cause reduced upper airway muscle tone and decrease ventilatory response to hypoxia, thus potentially increasing the AHI and prolonging apnea events. Recently, a Cochrane review found no worsening of OSA with most of the hypnotic and sedative drugs; however; decreases in minimum overnight SpO2 was observed. Testosterone replacement therapy (increases Apnea Hypopnea Index and prolonged hypoxemia time) has also been suggested to worsen OSA.

The medication which causes weight gain should also be avoided like atypical antipsychotics, antidepressants, anticonvulsants, etc [18]. In addition, there are several endocrine conditions that may present as OSA or may contribute to OSA. Thus, all initial evaluations of patients should include consideration of whether the patient has clinical signs and symptoms of hypothyroidism, acromegaly or Cushing's syndrome. Among these conditions, hypothyroidism is the most common (2% of adults), and its presentation may overlap with OSA symptoms: fatigue, weight gain, myalgias, memory loss, decreased libido, and depressed mood. Symptoms of OSA may improve by the treatment of the underlying endocrine disorder. The tricyclic antidepressant Protriptyline is the most effective drug studied in the treatment of OSA, Protriptyline produces its beneficial effect by stimulation of upper airway muscle tone and by decreasing the percentage of time spent in REM sleep, thereby reducing the more severe REM-related apneas. Another remarkable drug is Modafinil, a nonamphetamine CNS stimulant, which is used to reduce the daytime somnolence and increase alertness, but it is essential to understand that Modafinil cannot be used as a substitute for CPAP or an oral appliance. Additionally, Acetazolamide, a carbonic anhydrase inhibitor stimulates respiration by producing metabolic acidosis, thus, reduce the number of apneas and decrease the severity of oxygen desaturations in patients with OSA. Some patients with OSA benefit from the respiratory stimulant effect of progesterone, especially those with the obesity hypoventilation syndrome. Recently some studies have found that Bariatric surgeries lead to resolution/improvement of the patient's OSA, as measured by AHI.

2.4.5 Continuous Positive Airway Pressure (CPAP)

Continuous Positive Airway Pressure or CPAP is a modality of respiratory support in which increased pulmonary pressure is provided artificially during the expiratory phase of respiration in a spontaneously breathing neonate. Grunt in a baby with respiratory distress reflects an attempt to generate CPAP to keep alveoli open during expiration. CPAP is distinct from Intermittent Positive Pressure Ventilation (IPPV) or Intermittent Mandatory Ventilation (IMV) in which breathing is taken over by the ventilator machine completely and an increase in pulmonary pressure occurs during both inspiratory as well as expiratory phases. CPAP results in increased functional residual capacity (FRC) thus decreasing ventilation perfusion mismatch and better gas exchange. It results in splinting of upper airway thus decreasing airway resistance. These physiological effects result in decreased work of breathing and conservation of surfactant. However, excessive amount of CPAP can result in pulmonary air leaks and increase in pulmonary venous pressure. This can adversely affect the brain (increased risk of IVH) and heart.

An ideal CPAP delivery system mainly consists of a continuous supply of warm, gases supply, reservoir bag and blinder to mix the input gases (O2 and air). Figure 4 represent the main component of the CPAP system.

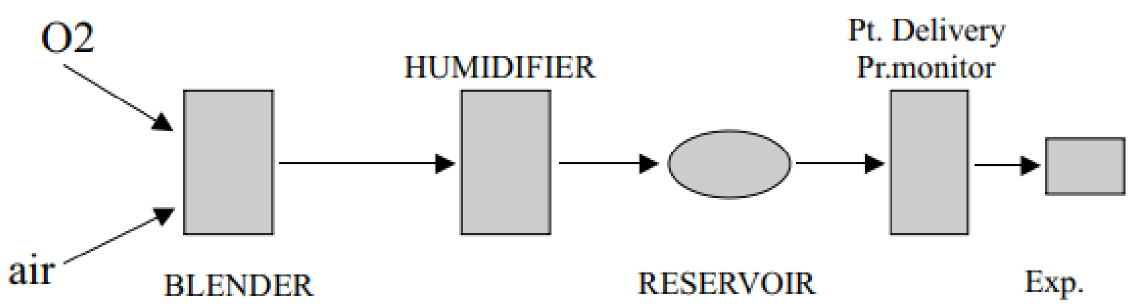

Figure 4 : CPAP system.

2.4.5.1 Types of CPAP based on gas flow

CPAP is divided in to two types depending upon type of flow viz. continuous flow and variable flow CPAP:

1. Continuous flow CPAP: In this type, a patient is provided a continuous fixed flow of gases irrespective of the phase of respiration. Ventilator derived

CPAP, conventional standalone CPAP machines and Bubble or water-seal CPAP are perfect prototypes.

2. Variable/Dual flow CPAP: Variable flow CPAP generates CPAP at the airway proximal to the patient's nares. It uses Bernoulli effect via dual injector jets directed towards each nasal prong in order to maintain constant pressure. If the patient needs more inspiratory flow, the venturi action of the injector jets entrains additional flow. Due to Coanda effect during spontaneous expiratory effort there is fluidic flip which causes flow to flip around and to leave the generator chamber via the expiratory limb. A residual gas pressure is provided by the constant gas flow, which enables stable gas delivery at a desired pressure during the entire respiratory cycle. The fluidic flip mechanism reduces the work of breathing almost to one fourth of the continuous flow CPAP in which neonate has to exhale against the full continuous flow of gas. It is also found that variable flow maintains better uniform pressure level than continuous flow. Still, cost and free availability are the limiting factors.

OSA patients wake up often throughout the night (although they may not remember doing so) and thus can be very tired during the daytime. In addition, each stoppage in breathing can lead to falls in oxygen level and a stress release of adrenaline, both of which can contribute to high blood pressure and put a strain on the heart. Left untreated, this situation can lead to serious health risk. Studies show that treatment of sleep apnea can make people feel better and reduce the risk of serious medical complications.

In general, CPAP technology delivers pressurized gas (blended air/oxygen) to the airway, through a mask or nasal cannula interface. For added benefit, the pressurized gas is humidified and warmed. Devices can be categorized into continuous flow and variable flow. The continuous flow devices provide a fixed flow of gases, and therefore pressure, regardless of the phase of expiration, while the variable flow devices exert a lower pressure during the expiratory cycle so that the infant does not need to exhale against a continuous flow of gases. v Bubble CPAP, a type of continuous flow device, uses a column of water to create continuous, end-expiratory pressures that are accompanied by fluctuations arising from the bubbling of air exiting the expiratory limb tubing. iv Research suggests that the vibrations that result from the bubbling help contribute to gas exchange and reduce the infant's work of breathing. vi When comparing the impact of CPAP devices, bubble CPAP has been demonstrated to be superior in terms of reduced complications, cost, and duration of hospital stay.

Figure 4: Continuous Positive Airway Pressure (CPAP).

Continuous PAP (CPAP), generally administered through the nose (nCPAP), is undoubtedly considered the gold standard treatment for OSA. Since its invention in 1983 by Dr Sullivan, the clinical application of this device has deeply modified the course of the disease over the last three decades, offering to thousands of patients the first noninvasive method to control their disorder. Worldwide, nCPAP is constantly recommended as the first-choice treatment for patients with moderate to severe OSA.

A CPAP of 7 to 15 cm of water acts as a pneumatic splint of the upper airway and prevents the passive collapse of soft tissues during respiration while sleeping. Stimulation of mechanoreceptors of the genioglossus muscle leading to increased airway tone has also been suggested as a mechanism of action. By this means.

Chapter Three
Background and Context

Chapter Three

Background and Context

Introduction

As discussed in the previous chapter, the known of respiratory rate of the OSA patient and the airway remains open is a very important It is very important for the patient to avoid many symptoms that may effect on his life. In this chapter, several background technologies and new technologies that is employed to achieve project aims, which is including respiratory rate sensor, Flexi-force sensor programmable microcontroller, and every things that is used in order to understand the behavior system.

3.1 Respiration Sensor

Breathing is one of the primary vital signs used to diagnose the health status of patients. Rate of respiration, together with heart rate, blood pressure, are used by healthcare workers to estimate the basic health-status of patients especially in the case of obstructive sleep apnea. In differentiating between stable and unstable patients, the rate of respiration is a better metric than other vital signs. Abnormalities in the rate and pattern of respiration are a strong predictor of acute events, such as obstructive sleep apnea, cardiac arrest, or for characterizing illnesses.

The strain gauge technique depends on a resistance change of the strain gauge that fixed on the patients thoracic as a belt. During patient's inhalation, the diaphragm contracts and will be pulled down, this increases the volume of the thoracic cavity. During exhalation, the abdominal muscle moves upward and pushes the diaphragm results in decreasing the thoracic cavity. The strain gauge monitors the changing of thoracic cavity volume during inhalation and exhalation. This technique is not comfortable for patients and requires a relatively sensitive strain gauge to obtain acceptable signal to noise ratio.

The thermistor technique is used to measure the temperature difference between the patient's exhaled air and the ambient environment by measuring of the thermistor resistance at each temperature. The temperature of the exhaled air is almost the same as that in the human body, whereas the temperature of the inhaled air is close to the ambient temperature. So the respiratory frequency can be obtained by putting a thermistor (such as NTC) close to patient's mouth to detect the change of temperature of inhaled and exhaled air. This technique has some problems; the signal to noise ratio of the output signal is relatively low, as a result further processing circuits are required such as differential amplifier, band reject filter, differentiator and hysteresis comparator. These electronic systems require large space in the board; make it not compatible for portable device, in addition to make it more expensive.

The thermometer technique is almost has the same procedure of the previous technique for obtaining the respiratory rate, but it is directly convert the change of air temperature to voltage. So this technique does not need any excessive components or stages, and also more accuracy than previous techniques. Thus the temperature sensor that is used for this purpose is DS18B20 digital thermometer. This sensor is suitable for this project due to its small size. It is cheap and has relatively high resolution, high accuracy, and can be powered from 3.3-5 volt.

3.1.1 Thermistor

A thermistor is a thermally sensitive resistor that exhibits a precise and predictable change in resistance proportional to small changes in body temperature. How much its resistance will change is dependent upon its unique composition. Thermistors are inexpensive, rugged, reliable and responds quickly. Because of these qualities thermistors are used to measure simple temperature measurements, but not for high temperatures.

The thermistor is used in this project to detect the patient respiratory rate and monitor the patient breathing , the thermistor will measures the temperatures of the exhalation and inhalation of the patient breath , so the resistance of the thermistor will change based on that will give us the breathing rate of the patient.

Thermistors, derived from the term thermally sensitive resistors, are a very accurate and cost- effective sensor for measuring temperature. Available in 2 types, NTC (negative temperature coefficient) and PTC (positive temperature coefficient), it is the NTC thermistor that is commonly used to measure temperature.

3.1.2 NTC Thermistor

An NTC thermistor is a thermally sensitive resistor whose resistance exhibits a large, precise and predictable decrease as the core temperature of the resistor increases over the operating temperature range. NTC thermistors are generally made of ceramics or polymers. Different materials used result in different temperature responses, as well as other characteristics.

While most NTC thermistors are typically suitable for use within a temperature range between −55°C and 200°C, where they give their most precise readings, there are special families of NTC thermistors that can be used at temperatures approaching absolute zero (-273.15°C) as well as those specifically designed for use above 150°C.

The temperature sensitivity of an NTC sensor is expressed as “percentage change per degree C”. Depending on the materials used and the specifics of the production process, the typical values of temperature sensitivities range from -3% to -6% per °C

3.1.3 Principle of thermistors work

The Thermistor (NTC) works on a simple principle: Change in temperature of the Thermistor, leads to a change in its resistance [20].

The resistance and temperature relationship can be approximated by the following equation:

$$R = R_0 e^{\beta}(\frac{1}{T} - \frac{1}{T_0}) \qquad 3.1$$

Where,

R = Resistance of Thermistor at the temperature T (in K).
R0 = Resistance at given temperature T0 (in K).
β = Material specific-constant.

In terms of temperature coefficient of resistance value at a certain temperature [26], Eq. (3.1) can be defined as:

$$R = R_0(1 + \alpha(T - T_0)) \qquad 3.2$$

The voltage drop across a thermistor increases with an increase in current as shown in Fig 3.1. The voltage increases until it reaches the peak value, after the peak value; it decreases with the increase in temperature.

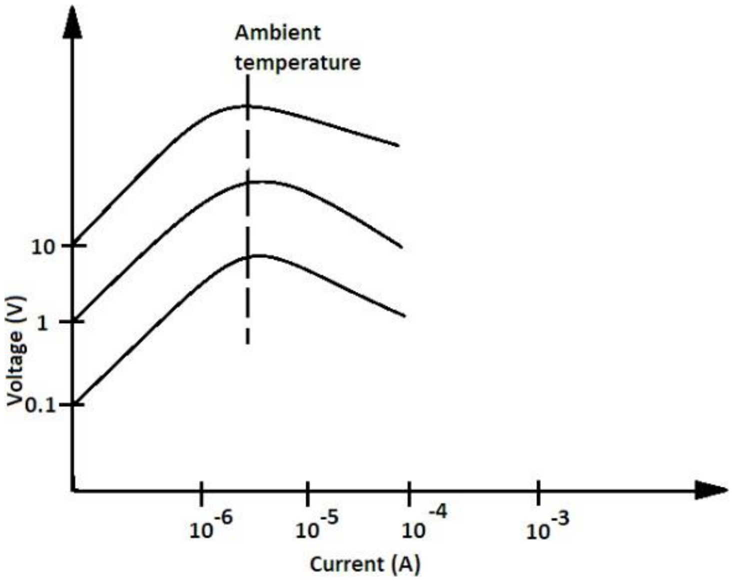

Figure 3.1 Voltage Current Characteristics [26].

This is so because, initially when an increase in the current is small, it is not able to produce a change in the temperature of the thermistor, therefore, the voltage drop across it increases. However, after the peak value, the value of the current is able to change the temperature of the thermistor. It increases its temperature. It results in a decrease in thermistor resistance. Hence, voltage drop across thermistor decreases.

3.2 Flexi-Force Sensor

The Flexi-Force sensor is an ultra-thin and flexible printed circuit, which can be easily integrated into most applications. With its paper-thin construction, flexibility and force measurement ability, the Flexi-Force force sensor can measure force between almost any two surfaces and is durable enough to stand up to most environments. Flexi-Force has better force sensing properties, linearity, hysteresis, drift, and temperature sensitivity than any other thin-film force sensors. The "active sensing area" is a 0.375” diameter circle at the end of the sensor.

The sensors are constructed of two layers of substrate. This substrate is composed of polyester film (or Polyimide in the case of the High-Temperature Sensors). On each layer, a conductive material (silver) is applied, followed by a layer of pressure-sensitive ink. Adhesive is then used to laminate the two layers of substrate together to form the sensor. The silver circle on top of the pressure-sensitive ink defines the "active sensing area." Silver extends from the sensing area to the connectors at the other end of the sensor, forming the conductive leads.

Flexi-Force sensors are terminated with a solder-able male square pin connector, which allows them to be incorporated into a circuit. The two outer pins of the connector are active and the center pin is inactive. Flexi-Force sensor acts as a variable resistor in an electrical circuit. When the sensor is unloaded, its resistance is very high (greater than 5 Meg-ohm), when a force is applied to the sensor, the resistance decreases.

3.2.1 Comparison between different types of Flexi-Force sensors

There are different types of Flexi-Force sensor that can used to measure the force of patient chest that affected from the respiratory system. The some properties of Flexi-Force sensor that illustrated in this section, The Flexi-Force A 401 is chosen according to its suitable properties for this device

3.2.2 The Flexi-Force A502

The Flexi-Force A502 is a square sensor, with a sensing area measuring at 50.8 mm x 50.8 mm (2 in. x 2 in.). This sensor is available off-the-shelf for easy proof of concept. The A502 can be used with our test & measurement, prototyping, and embedding electronics.

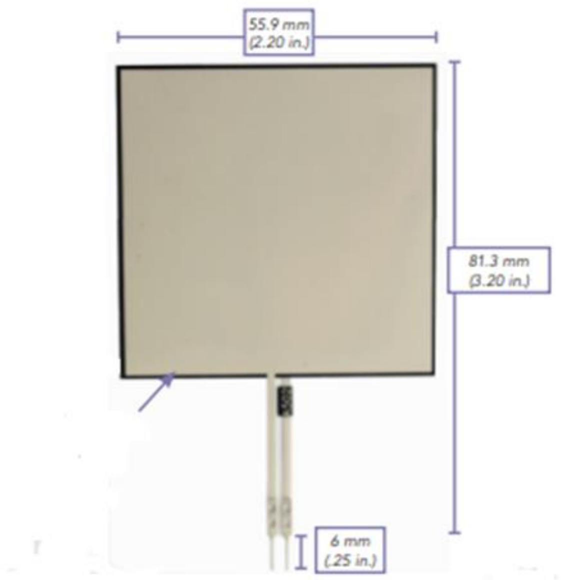

Fig3.2 Flexi-Force Sensor A502.

3.2.3 The Flexi-Force Sensor A401

The Flexi-Force A401 is piezo-resistive force sensor with the largest sensing area. It is available off-the-shelf for easy proof of concept and is available in large volumes for design-in applications. The A401 can be used with test & measurement, prototyping, and embedding electronics,

Flexi-Force A401 can measure up to 31,138 N (7,000 lb). The force range can be extended by reducing the drive voltage, VT, or the resistance value of the feedback resistor, RF. Conversely, the sensitivity can be increased for measurement of lower forces by increasing VT or RF.

Fig3.3 FlexiForce Sensor A401.

3.2.4 Physical properties of A502 FlexiForce sensor

1. Thickness 0.203 mm (0.008 in.)
2. Length 81.3 mm (3.20 in.)
3. Width 55.9 mm (2.20 in.)
4. Sensing Area 50.8 mm x 50.8 mm (2 in. x 2 in.)
5. Connector 2-pin Male Square Pin
6. Substrate Polyester
7. Pin Spacing 2.54 mm (0.1 in.) [11]

3.2.5 Typical performance of A502 FlexiForce sensor

1. Linearity (Error) < ±3% of full scale
2. Repeatability < ±2.5%
3. Hysteresis < 4.5 % of full scale
4. Drift < 5% per logarithmic time scale
5. Response Time < 5µsec
6. Operating Temperature -40°C - 60°C (-40°F - 140°F)

3.3 Microcontrollers Unit.

A microcontroller is a highly integrated chip that contains all the components comprising a controller, this includes a CPU, RAM, some form of ROM, I/O ports, and timers, and a microcontroller is a small computer on a single integrated circuit containing a processor core, memory, and programmable input/output peripherals.

As microcontroller is an integrated circuit, the cost of the total system decreases, a smaller and cheaper circuit board used, the labor required to assemble and test the circuit board reduces, and the number of chips and the amount of wiring reduces. Microcontrollers are designed for using in embedded systems, which mean that they are part of embedded systems, so they are sometimes called "embedded microcontrollers".

A microcontroller is designed for a very specific task to control a particular system and is used in automatically controlled products and devices, such as automobile engine control systems, implantable medical devices, remote controls, office machines, appliances, power tools, and toys. By reducing the size and cost compared to a design that uses a separate microprocessor, memory, and input/output devices, microcontrollers make it economical to digitally control even more devices and processes.

Most microcontrollers deal with a digital data, so analog-to-digital converter (ADC) must be exist to convert analog data to digital, but in some microcontrollers there is a digital-to-analog converter (DAC) that allows the processor to output analog signals or voltage levels.

There are many microcontroller types and architectures different in length of register and instruction word. We can mention here the most known types of microcontrollers:

- PIC (8-bit PIC16, PIC18, 16-bit dsPIC33/PIC24)
- Intel 8051
- Arduino
- AT mega

The microcontroller that used in this project is arduino (Mega and Uno) microcontroller. Arduino is an open-source physical computing platform based on a simple microcontroller board, and a development environment for writing software for the board. Arduino can be used to develop interactive objects, taking inputs from a variety of switches or sensors, and controlling a variety of lights, motors, and other physical outputs. The main advantages of arduino microcontrollers:

- Inexpensive - Arduino boards are relatively inexpensive compared to AT mega microcontroller platforms.
- Simple, clear programming environment - The arduino programming environment is easy-to-use for beginners, yet flexible enough for advanced users.
- Open source and extensible software- The arduino software and is published as open source tools, available for extension by experienced programmers.
- Open source and extensible hardware - The arduino is based on Atmel's ATMEGA8 and ATMEGA168 microcontrollers.

There are several kinds of PIC which is largely similar in hardware: Arduino Mega, ArduinoUno and Arduino Nano.

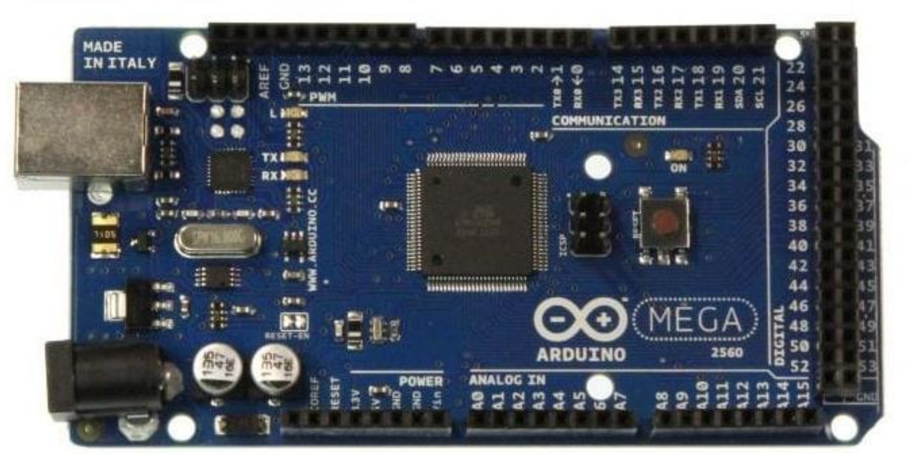

Figure 3.4: Arduino Mega Microcontroller.

3.4 Bluetooth HC-05 circuit

HC-05 Bluetooth Module is an easy to use Bluetooth SPP (Serial Port Protocol) module, designed for transparent wireless serial connection setup. Its communication is via serial communication which makes an easy way to interface with controller or PC. HC-05 Bluetooth module provides switching mode between master and slave mode which means it able to use neither receiving nor transmitting data.

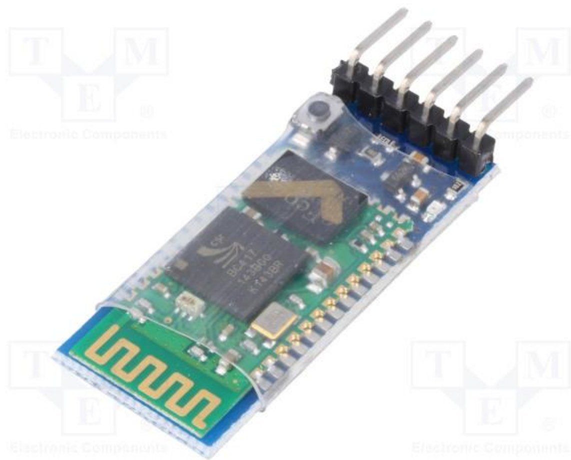

Figure 3.5: Bluetooth HC05 circuit.

3.5 Display Circuit

The LCD display Module is built in a LSI controller, the controller has two 8-bit registers, an instruction register (IR) and a data register (DR). The IR can only be written from the MPU. The DR temporarily stores data to be written or read from DDRAM or CGRAM. When address information is written into the IR, then data is stored into the DR from

DDRAM or CGRAM. By the register selector (RS) signal, these two registers can be selected.

It's easily controlled by MCU such as 8051,PIC,AVR,ARDUINO,ARM and Raspberry Pi.It can be used in any embedded systems,industrial device,security,medical and hand-held equipment.

The display device that will be used in the project is LCD (4*16); it can display sixteen characters on four rows which is very good for the project. The data displayed on the LCD are heart rate, respiration rate , movement rate every 3 hours , and if there is an abnormal values it will displayed on LCD show the value that is abnormal.

Figure 3.6 LCD.

3.6 Alarm Circuit

Alarms are intended to draw attention to a problem before it harmful. Most stand-alone monitors can generate an alarm when a monitored variable crosses fixed or adjustable limits.

Alarms with this design are used to warn the patient and patient‟s family, that there is something wrong in breathing, heart beating or in patient movement while sleeping.

3.6.1 Buzzer

A buzzer or beeper is an audio signaling device, which may be mechanical, electromechanical, or piezoelectric. Typical uses of buzzer and beepers are as alarm devices. A buzzer is an integrated structure of electronic transducers, a DC power supply, widely used in computers, printers, copiers, alarms, electronic toys, automotive electronic equipment, telephones, timers and other electronic products needing sound devices. Here it is used when something get wrong with one of the parameters In this situation the buzzer is chosen with the criteria of the sound not being too high and its voltage trigger must also be suitable for the output voltage Arduino hardware (see figure) a voltage is 5 volt DC.

Figure 3.7 Types of buzzer [33].

3.6.2 LED

Light Emitting Diode is a very important meric of the conversion of electrical energy into emitted optical energy.LEDs produce more light per watt than incandescent bulbs;this is useful itn battery powered or energy saving devices, LEDs can emit light of an intended color without the use of color filters that traditional lighting methods require. This is more efficient and can lower initial costs. LEDs can have a relatively long useful life. LEDs have a life time of about 50,000 hours, whereas Fluorescent tubes typically are rated at about 30,000 hours, and incandescent light bulbs at 1,000-2,000 hours. In this project two colors used red for danger situation when something wrong happened with one of the parameters. Figure 3.10 shows sevsral LEDs.

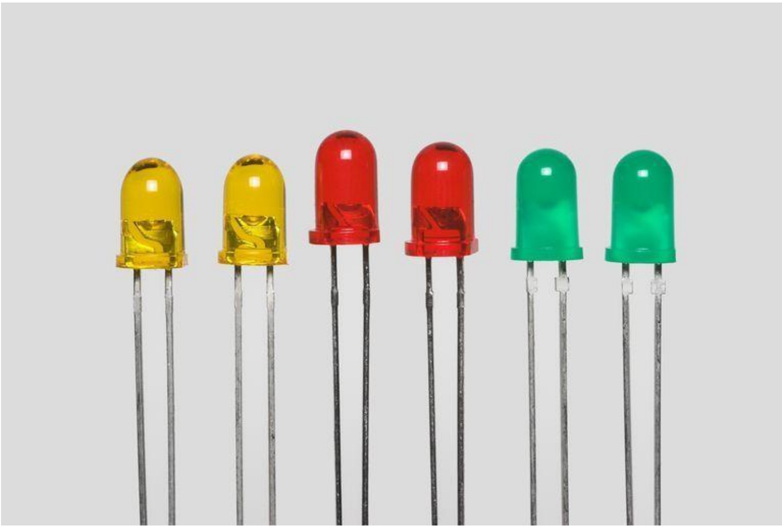

Figure 3.8 Types of LEDs .

Chapter Four
System Design

Chapter Four

System Design

This chapter talks about the system design including all the hardware and software components required. Each stage of the system will be explained in detail, the hardware components of each stage are chosen carefully to achieve the desired objectives.

The main system architecture is depicted in figure (4.1); it is composed of two main parts; sensing and processing parts. The sensing part contains a respiratory rate sensor to measure the respiratory frequency, and Flexi-Force sensor to sense the motion of the patient chest. The main functions of the processing parts are receiving data from the sensing parts and process the output signal processing of each sensor, and send the results to the Microcontroller to analyze, compare with standard values, and display it using display device or send the result via bluetooth. A rechargeable 9-V battery supplies the overall system.

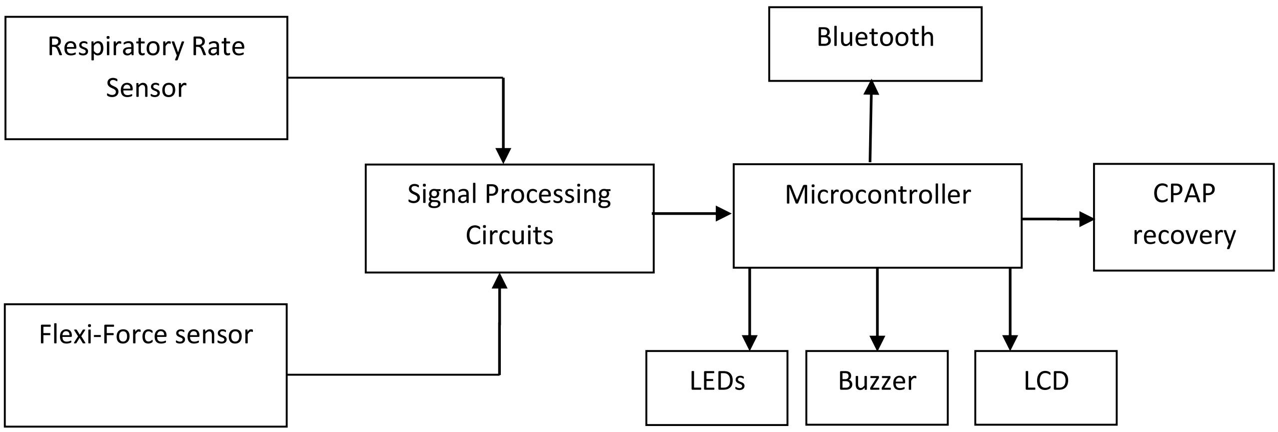

Figure 4.1: Main Block Diagram for the System.

An explanation of each stage within the system is given in the following sections.

4.1 Design of Respiratory Rate Measurement

The respiratory rate sensor is used to count the number of patient's breath per minute, which is achieved by measuring the temperature difference between human body (37℃) and ambient temperature. The output signal is processed through different stages and then sent to the microcontroller to analyze it and print the result on the display device as shown in Fig. 4.2.

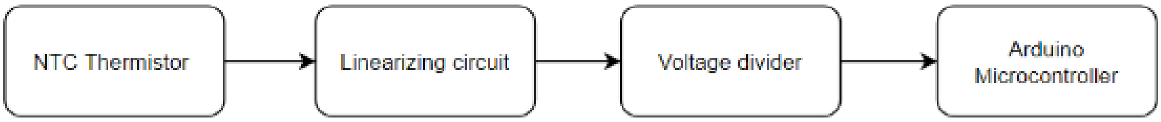

Figure 4.1: Main Block Diagram for Respiratory Rate Measurement Circuit.

4.1.1 Thermistor NTC Sensor.

Most thermistors are highly non-linear over a wide operating temperature range. In many cases, thermistor linearization over a wide temperature range proves to be a challenge. The principle of the linearization circuit is to transform the nonlinear thermistor's resistance-temperature change into a linear voltage-temperature dependency. The accuracy of such transformation depends on many factors including, the circuit itself, the circuit component values, and the linearizing temperature range, so the accurate temperature measurements had to be secured through the development of proper circuits with optimal component values.

Figure 4.3 shows the response of a NTC thermistor between -40°C and 60°C. From the figure you can see that thermistors have high sensitivity. A small change in temperature causes a large change in resistance. Also note that the response of this thermistor is not linear. That is, the change in resistance for a given change in temperature is not constant over the thermistor's temperature range.

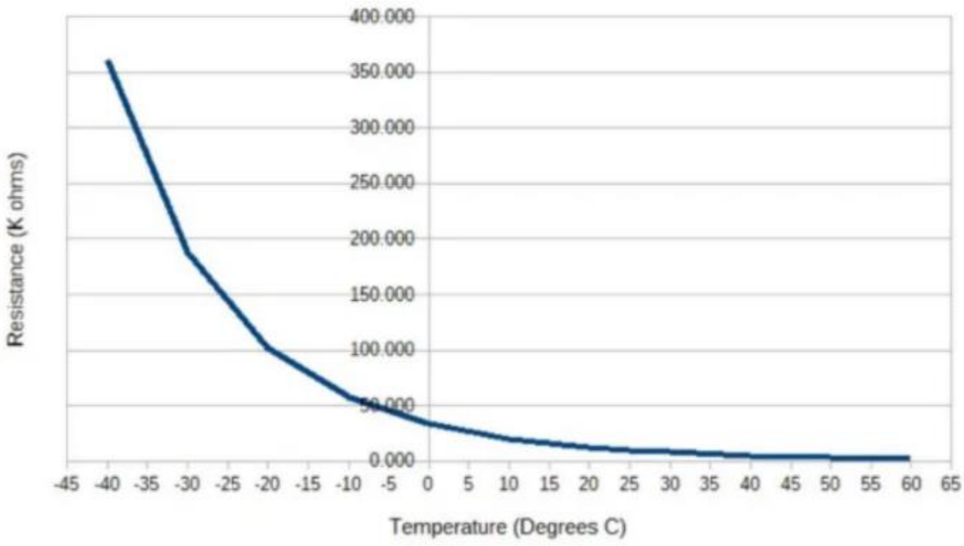

Figure 4.3: Thermistor temperature-resistance curve -40°C to 60°C.

The manufacturer's data sheet includes a list of thermistor resistance values and corresponding temperatures over its range. The linearizing of the NTC sensor is produced by placing a 10K resistor in parallel with a thermistor whose resistance is 10K at 25°C as illustrated in Figure 4.4. This makes the region of the curve between 0°C and 50°C fairly linear.

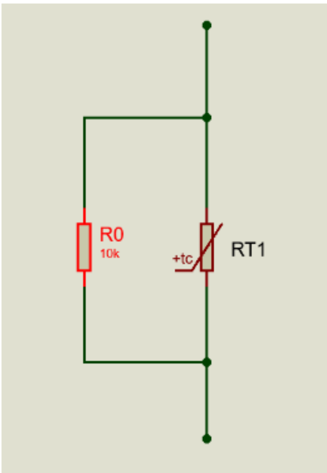

Figure 4.4: Thermistor Linearizing Circuit.

4.1.2 Voltage Divider.

A common way for capturing the analog data by the Arduino microcontrollers is via an analog to digital converter (ADC) after linearizing the sensor. Arduino microcontroller can not directly read the thermistors resistance with an ADC. The series thermistor-resistor combination, shown in Figure4.5, provides a simple solution in the form of a voltage divider.

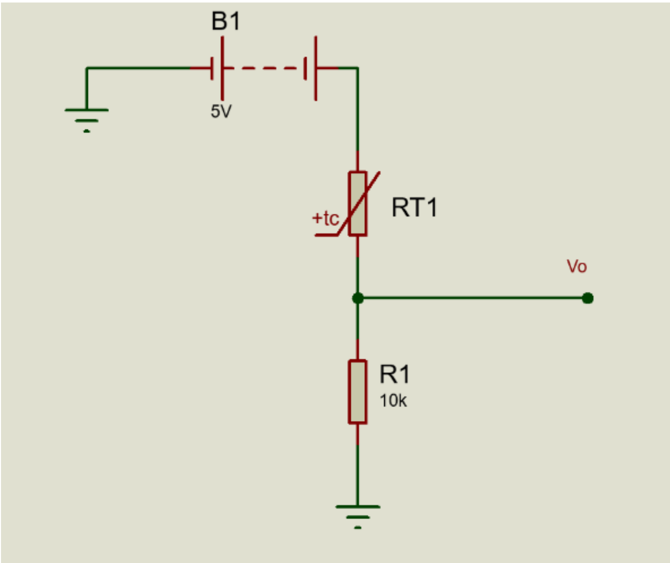

Figure 4.5: Thermistor voltage divider.

The following formula can be used to calculate the voltage divider output voltage:

$$V_o = 5\left(\frac{R_1}{R_1 + R_{T1}}\right) \quad \textbf{4.1}$$

The linearized temperature-voltage curve in figure 4.6 shows the change in voltage divider output voltage Vo in response to temperature change. The source voltage B1 is 5 volts, the thermistor resistance RT1 is 10K ohms at 25°C, and series resistor R1 is 10K ohms. This combination has maximum linearity around the mid point of the curve, which is at 25°C.

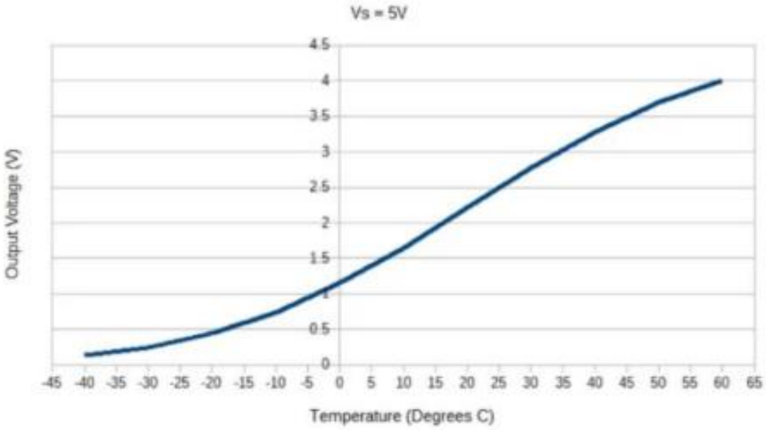

Figure 4.6: Temperature-voltage curve.

To convert ADC data of the thermistor NTC sensor to temperature, we need to find the thermistor resistance and then use it to find the temperature. Eq. 4.1 becomes:

$$R_{T1} = R_0(\frac{5}{V_o} - 1) \qquad 4.2$$

In Arduino microcontroller, the ratio of voltage divider input voltage to output voltage is the same as the ratio of the ADC full range value (adcMax) to the value returned by the ADC (adcVal), so when we use a 10 bit ADC then adcMax is 1023.

Now you can replace the ratio of voltages with the ratio of ADC values in the equation to solve for RT1:

$$R_{T1} = R_0(\frac{AdcMax}{AdcVal} - 1) \qquad \mathbf{4.3}$$

Once we calculate the value for RT1, we can use a saved table in the Arduino microcontroller that containing temperature-resistance data for our NTC thermistor to find the corresponding temperature.

4.2 Flexi-Force Sensor

Flexi-Force sensor is used to sense the motion of patient chest to alarmed if there occlusion in the airflow during sleep. Flexi-Force sensor is a polymer thick film (PTF) sensor that exhibits a decrease in resistance with an increase in the force applied to the active surface. Its force sensitivity is optimized for use in human touch control of electronic devices. Flexi-Force sensor is not a load cell or strain gauge, though they have similar properties. The following block diagram describe the procedures of processing the signal that come from Flexi-Force sensor.

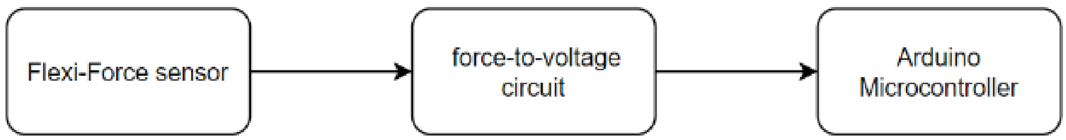

Figure 4.7: Main Block Diagram for Flexi-Force Circuit.

4.2.1 Force-to-Voltage circuit

Flexi-Force sensor acts as a variable resistor in an electrical circuit. When the sensor is unloaded, its resistance is very high (greater than 5 Meg-ohm); when a force is applied to the sensor, the resistance decreases. The following graph displays the resistance and Conductance Vs force curve for the Flexi-Force A402 sensor.

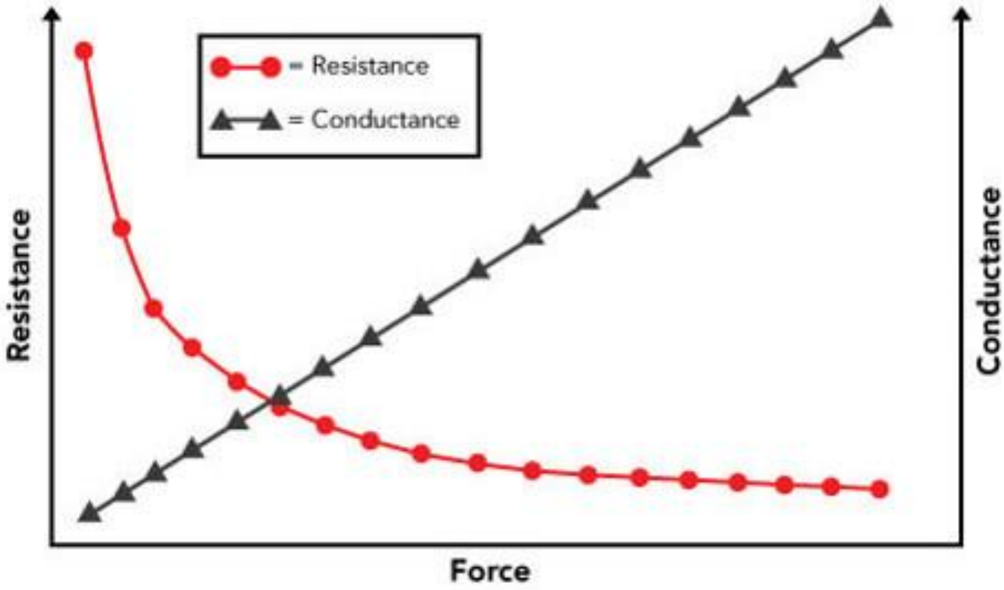

Figure 4.8: Resistance and Conductance Vs Force curve for FSR 402

When we applied a force on a Flexi-Force sensor, the value of output resistance form the sensor will be decreased. The multimeter can be used to measure the value of resistance. When a force is applied to the sensor the output resistance decreasing, the resistance can be read by connecting a multimeter to the two sensor's pins then applying a force to the sensing area. The conductance for this sensor distinguishes that it has a linear relationship with the applied force Linearity are presented in Table 4.1.

Table 4.1 Force-Resistance Relation

Force(lbs)	Resistance(KΩ)
0.5	924.57
1	711.21
5	390.24
10	206.16
20	103.08
30	68.72
34.28	60

Since Flexi-Force sensor acts as a variable resistance and it is change in accordance with input applied force, so we need to use a force to voltage circuit to convert the force that applied on the sensor to a voltage that can easy to deal. Figure 4.9 represent a force to voltage circuit that is used in this project, where an AD822AN operational amplifier is chosen because of it is advantage (single power supply, rail to rail and wide input voltage range(3-36 V) and suitable for medical instrumentation and application.).

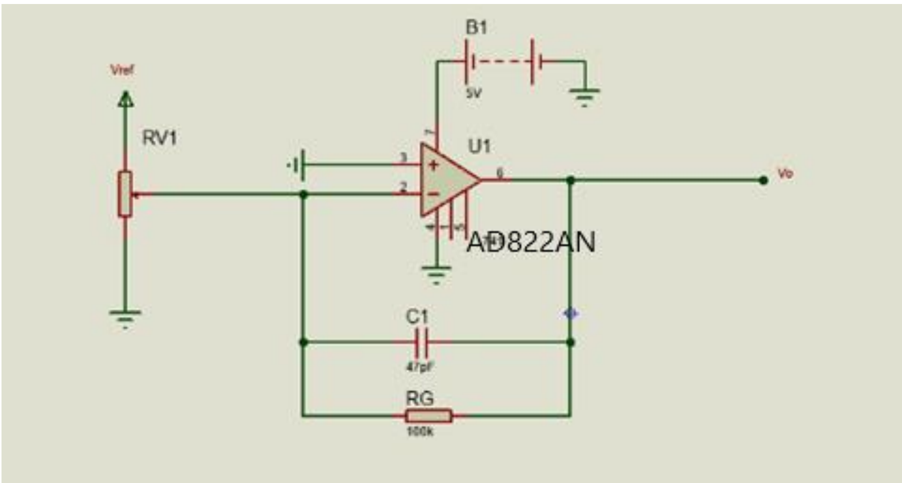

Fig 4.9: Force to Voltage Circuit

AD822AN was connected as inverting op-amp to produce more linear output voltage than non-inverting op-amp, to obtain 5 volt as maximum output voltage, feedback resistance should be adjusted as (RG= 100KΩ) as illustrated in Eq. 4.4.

To calibrate 5 output voltage at maximum load (34 Ib) with an input of (-3 volt), the sensor resistance will reach approximately (60KΩ) as illustrate in table 4.1. The gain resistance can be calculated as follow:

$$Vout = -Vin * \frac{RG}{RV1}$$

$$RG = Vout * \frac{RV1}{-Vin} \quad 4.4$$

$$RG = 5\,V * \frac{60K\Omega}{-(-3V)}$$

$$RG = 100K\Omega$$

Where Vin=-3 volt, RG= 100KΩ, and RV1 as shown in table 4.1, the approximated value of output voltage can be calculated as illustrated in table 4.2, where 1lb=0.45kg and 1lb=4.448N

Table 4.2: Force to voltage relations.

Force(lbs)	Vout (volt)
0.5	0.324
1	0.423
5	0.768
10	1.455
20	2.910
30	4.365
34.28	5.010
40	5.835

4.3 Arduino Interfacing

An Arduino Mega acquires the Flexi-Force, respiratory rate and heart rate signals via "digital and analog" pins on the Arduino mega board. It processes the different signals, display the result on LCD, and activate alarm system. It has 55 digital input/output pins and 15 analog input pins and powered by 5V. Flexi-Force, respiratory rate and heart rate systems outputs are connected to the arduino mega through the serial data line ANALOG A0, ANALOG A1 and ANALOG A2 pin on the arduino mega board, as shown in figure 4.10.

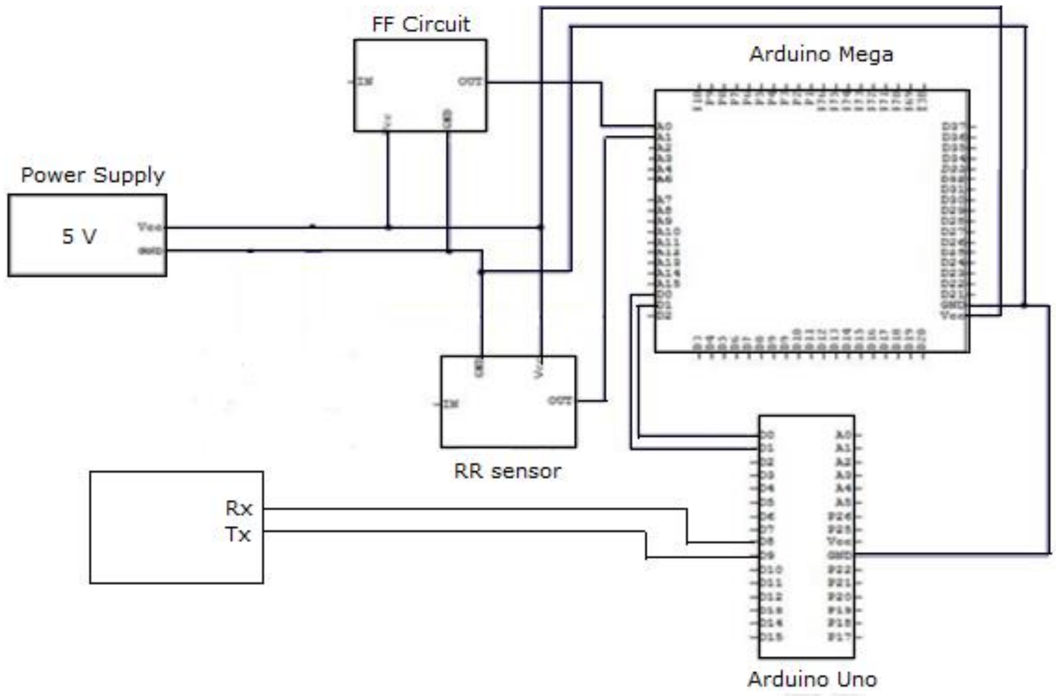

Figure 4.10: Arduino Mega Interfacing with Respiratory Rate and Flexi-Force and another Arduino Uno.

Arduino Uno is chosen to receive all the data from Arduino Mega Flexi-force sensor, then analyze the data that received and comparing it with a data that saved preciously in the Arduino Uno. The arduino Uno and mega were connected together through serial communication using pins (RX0-TX1, RX1-TX0).

4.4 LCD Display

The display device that used in the project is LCD (4*16); it can display sixteen characters on four rows which is very good for the project. The data that displays on the LCD are hear rate, respiratory rate, the number of chest motion with general heath condition (emergency case and normal case).

4.5 Alarm System

The alarm system consists of three LEDs (yellow, Green and red) and a buzzer. The yellow LED is ON during the controller processing. The green LED will be ON when the diagnostic result within the normal range. The red LED and the buzzer will be ON when the diagnostic result is out of the normal range.

This alarm will be is Audio and Visual alarm by using the ARTC 4330 buzzer audio and using the led with red color to attenuate the patient in wrong case, the connection and circuit of buzzer and led show in Figure 4.11 and 4.12.

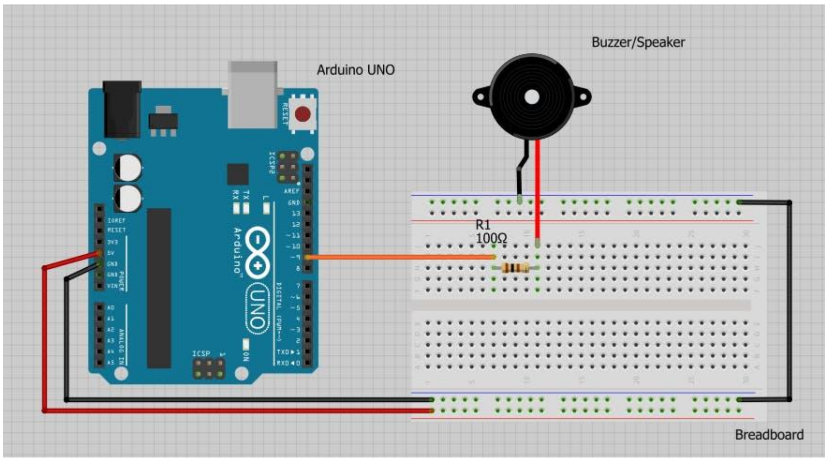

Figure 4.11: buzzer connection with Arduino.

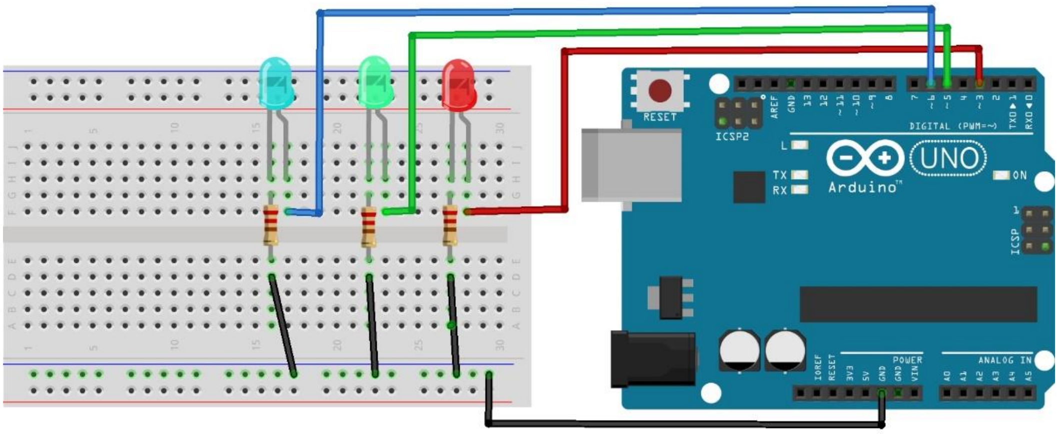

Figure 4.12: LED's connections with Arduino.

4.6 Bluetooth System

HC-05 Bluetooth Module is used in this system to send the analyzed data from Arduino Uno to application that installed on the doctor or any related person, the data send via serial port

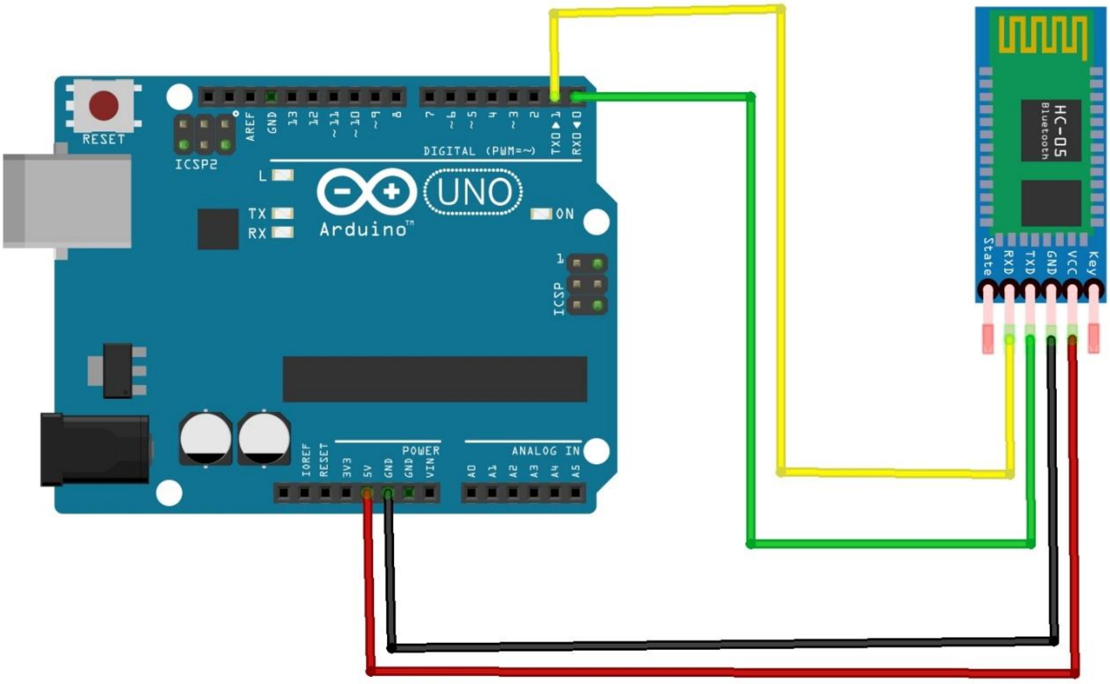

Figure 4.13: Bluetooth connections with Arduino.

4.7 Power Design

The hardware system needs power supply to provide its components with the required power. As the system is required to be portable a battery that has the following characteristics is required:

1. Light weight.
2. Provide required system power.
3. Has relatively long life.

Due to limitation of power supply in the system, choosing of system parts should fulfill the need for an optimal with minimum current consumption leading to increase the life time of the battery. The system intended to operate using a rechargeable (9- volt) battery, but all stages need to operate within a voltage supply of (5) volt. This stage uses voltage regulator (LM317) to obtain these voltage values from the battery keeping in mind the current consumption of all electrical parts used in the system. Table (4.2) explain the name of different parts used in the system with the power consumption relate to each one to find the overall system current consumption and verify that the power source able to give this desired value, also calculate the expected life time for the battery.

Table (4.2): Current Consumption of the Internal System Components.

Part Number	Function	Quantity	Current Consumption
LMC662	OP-Amp	4	0.75mA*4=3mA
TCRT1010	Phototransistor	1	150mA
2N3904	Transistor	1	170mA
Arduino Mega	Output Pins	15	20mA*15=300mA
Arduino Uno	Output Pins	7	20mA*7=140mA
LCD	Display	6	5mA*6=30mA
LED	Display	3	20mA*3=60mA
Flexi-Force	Sensor	1	250mA

DS18b20	Temperature sensor	1	5mA
Total Current Consumption		1120mA	

After this estimation about the expected current and voltage values of all system components, now it's important to choose the power supply parameters to meet these requirements reaching to optimal system operation. Polymer-Lithium 9v rechargeable battery with (2100mA/h) current capability, this battery is good enough to supply the portable system with its required power.

Figure 4.14 shows the schematic electrical connection of voltage regulator to obtain (+5v).

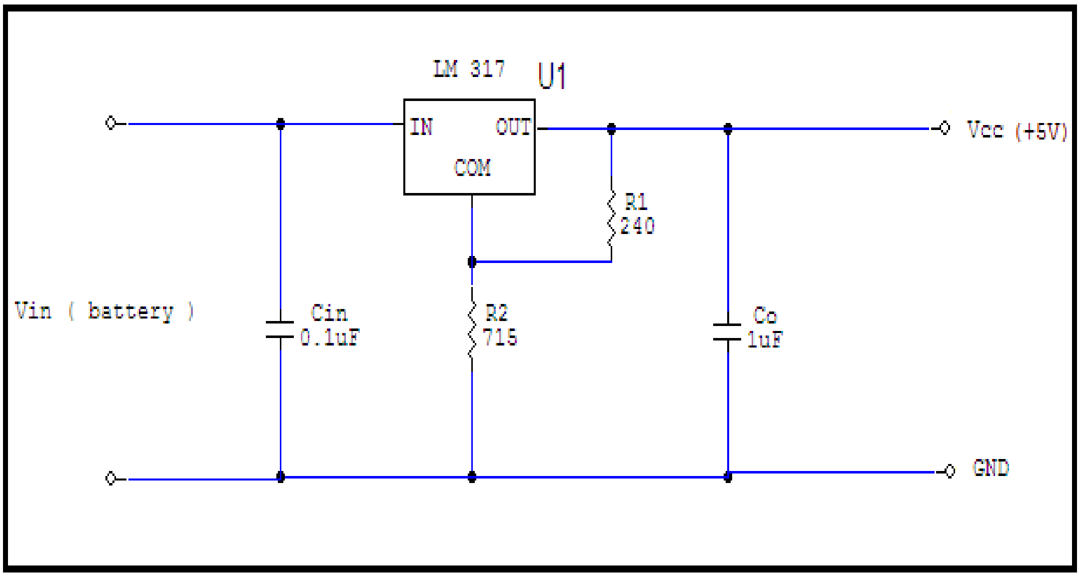

Figure 4.14: Circuit Diagram of Power Supply.

LM317 (U_1) was chosen as positive voltage regulator due to its relatively high output current capability (1.5A), adjustable output voltage, and low cost features. Desired output voltage can be computed according to the following formula:

$$V_{out} = 1.25V\left(1 + \frac{R_2}{R_1}\right) + I_{adj}R_2 \qquad \textbf{4.5}$$

According to U_1 datasheet [Appendix-E], R_1, C_{in}, and C_o equal 240Ω, 0.1µF, and 1µF respectively. R_2 was adjusted to obtain 5v output voltage, also I_{adj} is controlled to less than 100µA, and the error associated with this term is negligible in most applications. Hence, substituting I_{adj} by 100µA into Eq. 4.5 results in 5V output voltage as follows:

$$\mathbf{5 = 1.25v^{*}\left(1 + \frac{R2}{240}\right) + 100\ \mu A^{*}R2} \qquad \textbf{4.6}$$

Solving equation (4.3) for R_2, obtaining $R_2 = 715\ \Omega$.

|

Chapter Five
System Implementation

Introduction

In this chapter, the hardware system designed in the preceding chapter is implemented to accomplish the project as a one unit which achieves the purpose of the project. In this section, subsystems circuits will implemented before final implementations to the system.

5.1 Project Implementation

The temperature sensor has to be close enough to the patient's breath; therefore this sensor was located in a mask. The mask that used is made by a reinforced rubber material which is suitable for the patient's face. The mask used in this project is shown in figure (5.1).

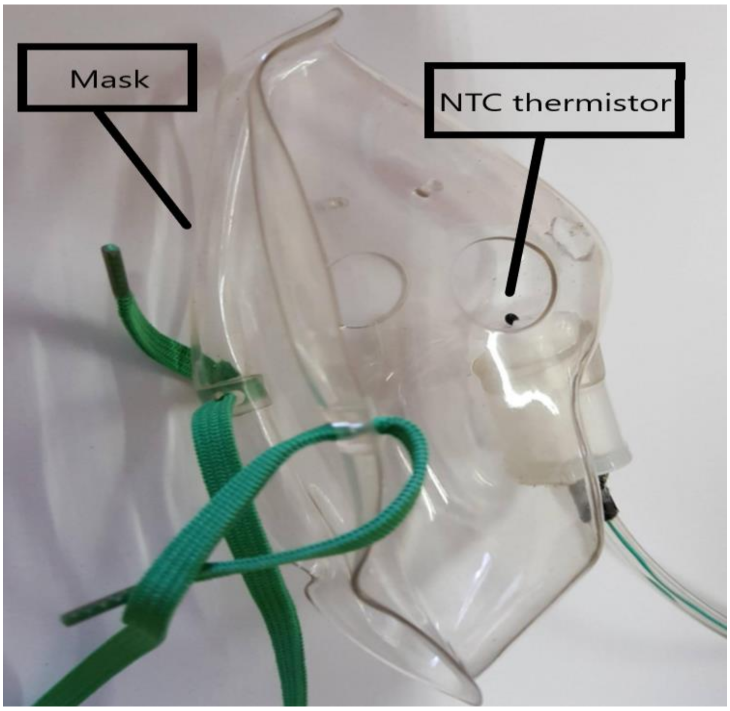

Figure (5.1): Mask and its NTC Temperature Sensors.

5.1.1 Respiratory Rate Measurement Circuit

The temperature sensor used in the respiratory circuit needs calibration in addition to software programming. It is calibrated, tested and programmed on the Arduino as shown in figure (5.2).

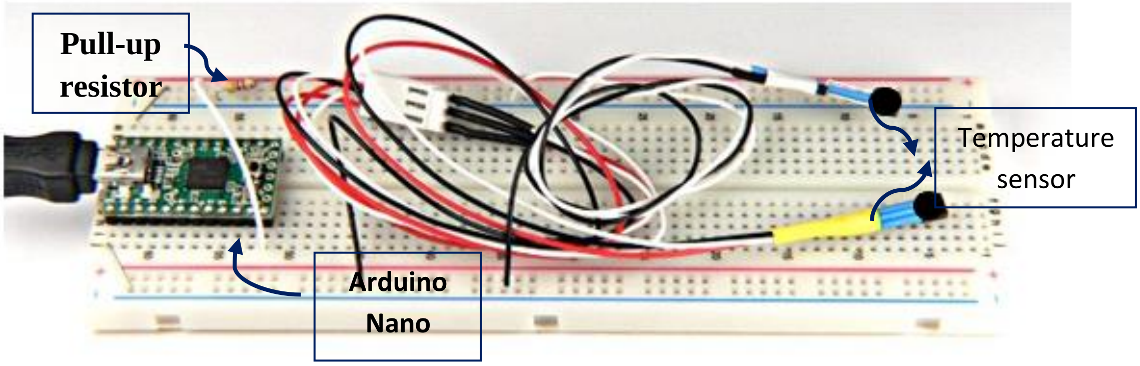

Figure (5.2): Temperature Sensor Circuit.

After programming the sensor, it is fixed on the mask and connected to the Arduino mega to measure the temperature of patient's breath as discussed in the previous chapter.

5.1.2 Flexi-Force Sensor:

The Flexi-Force sensor circuit consists of Flexi-Force sensor and processing circuit. The two of Flexi-Force sensor is located on a shirt to detect the moving of patient chest. The processing circuit is located in the system box. It composed amplification and filtration circuits as illustrated in figure (5.3).

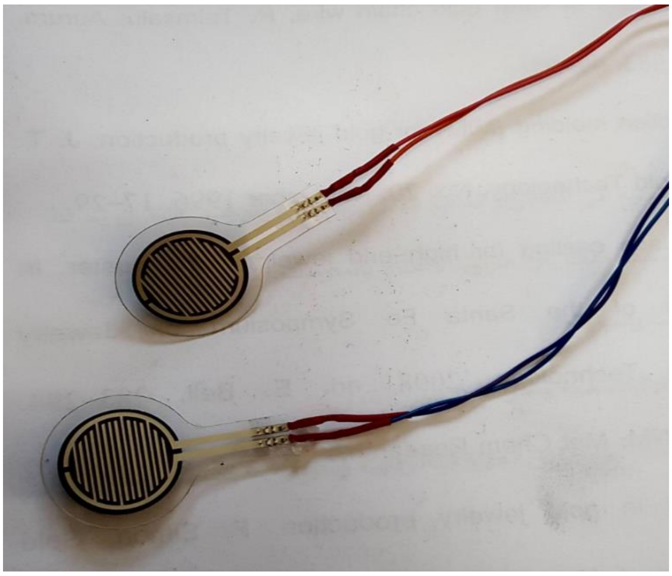

Figure (5.3): Flexi Force Circuit.

5.1.3 Controller Connections

As mentioned in the previous chapter, the Arduino Mega is the brain of the project, temperature circuit, LCD, LEDs, Arduino Uno and buzzer are connected to it. Where the Arduino Uno is used to measure the movement of the chest, then send the data stimuonesly to Arduino Mega. The connection of Arduino is illustrated in Figure 5.4. section will show these connections in the following figure (5.5)

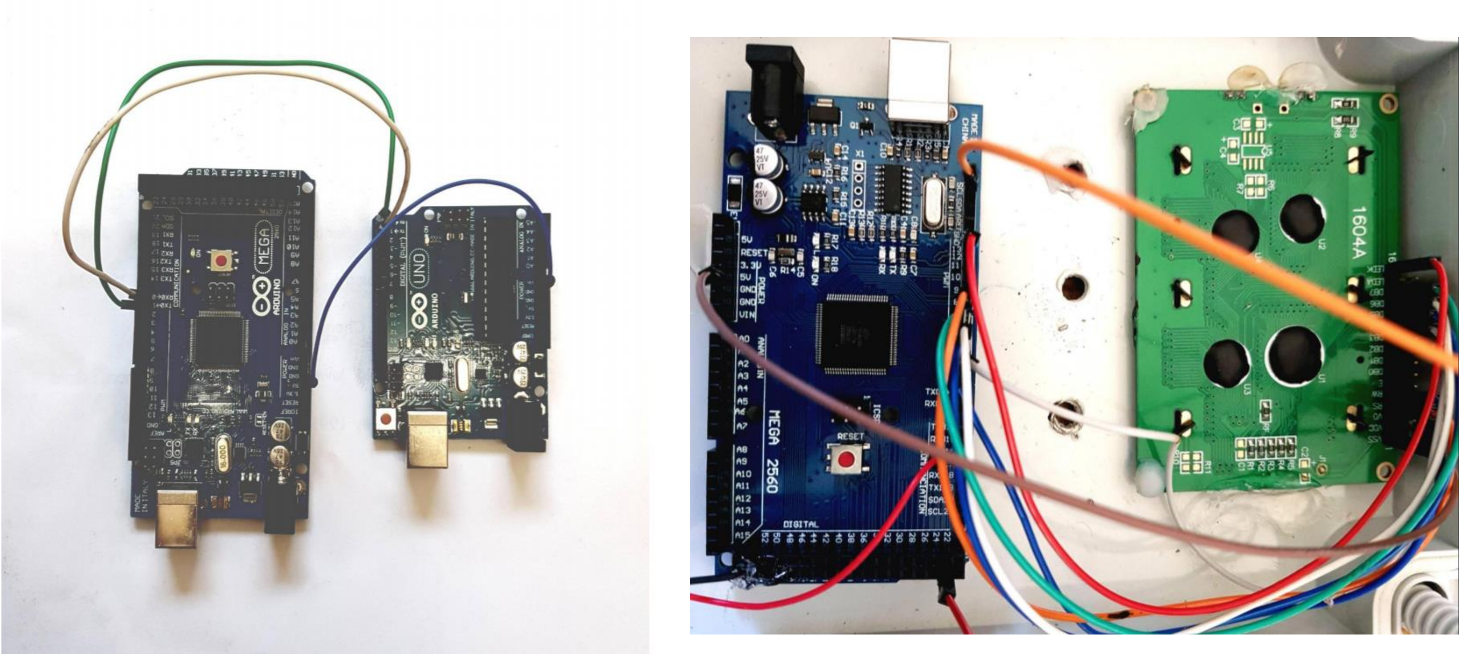

Figure 5.4: Arduino microcontroller connections.

5.1.4 Power Supply Circuit:

As mentioned in the previous chapter, the power supply circuit is used to provide the required voltage (5V) to the other circuits and subsystems. Figure (5.5) shows power supply circuit and its components.

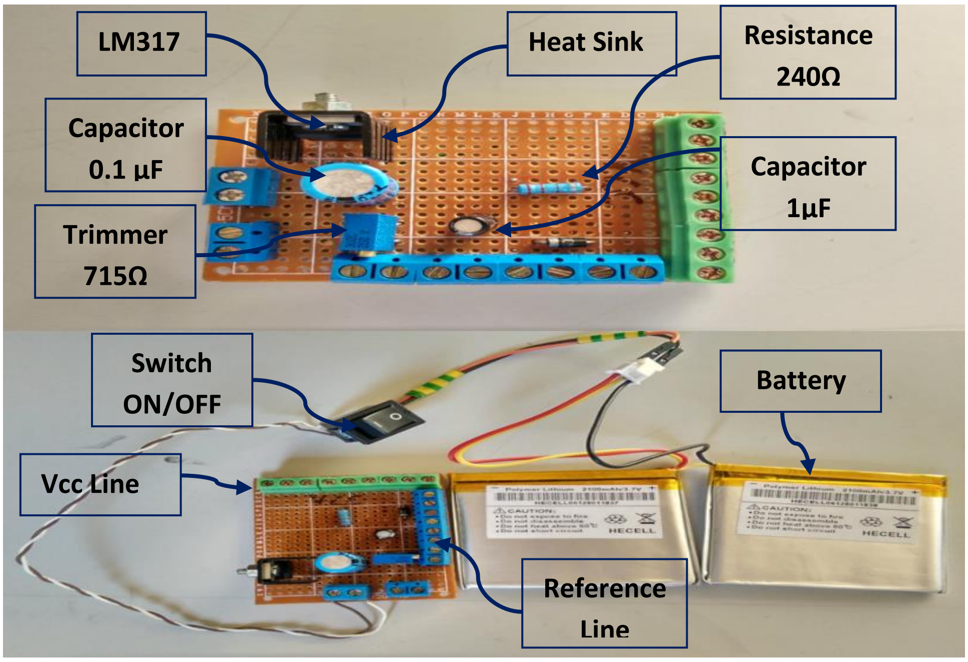

Figure (5.5): Power Supply Circuit.

Chapter Six
Results and Conclusions

6.1 Results

After the project is installed, its readings are examined on ten persons. The result of all readings is approximately close to the real readings. Table (6.1) shows these readings.

Table (6.1): The Table of the Result.

#	Respiratory rate (RPM)	Number of chest movement	Statues of the patient
1	14	11	Good
2	15	12	Good
3	21	14	Good
4	16	12	Good
5	17	13	Good
6	19	15	Good
7	14	14	Good
8	17	11	Good
9	18	14	Good
10	15	13	Good

The case of OSA was tested virtually by removing the mask and Flexi-Force sensor form the patient, and running the device freely without patient. The device detect the OSA case and run CPAP device for recovering the patient.

6.2 Challenges

While designing the system, there are many challenges have been faced, such as:

- Some of the project components are expensive such as CPAP device.
- The Arduino mega couldn’t used for parallel data reading from the sensors.

6.3 Conclusions

The CO respiratory rate and Flexi-Force sensors are used to indicate a very important physiological signs that help patient with OSA case to treat with it. After designing, processing, implementing and testing these sensors, the overall system can provide the following features:

- In this project a diagnostic system has been built using respiratory rate sensors and Flexi-Force sensors to detect the OSA case.
- The respiratory rate and Flexi-Force sensors are designed to measure continuously.
- The box design was light as possible and combined between beauty and efficiency.

6.4 Recommendations

In this project, the system was designed to detect the OSA case by detecting a various physiological signs such that respiratory and chest movement, but these signs are not sufficient to give the exact total diagnostic, so this project needs more research time to improve its efficiency and some features could be added like acetone sensor when it is available commercially. Also for future works, the telemedicine property and feature can be used to remotely diagnose, treat, and manage the care of OSA patients.

Appendix - E

LM 317

September 2014

KA317 / LM317
3-Terminal Positive Adjustable Regulator

Features

- Output-Current In Excess of 1.5 A
- Output-Adjustable Between 1.2 V and 37 V
- Internal Thermal Overload Protection
- Internal Short-Circuit Current Limiting
- Output-Transistor Safe Operating Area Compensation
- TO-220 Package

Description

This monolithic integrated circuit is an adjustable 3-terminal positive-voltage regulator designed to supply more than 1.5 A of load current with an output voltage adjustable over a 1.2 V to 37 V range. It employs internal current limiting, thermal shutdown, and safe area compensation.

TO-220

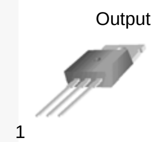

1. Adj 2. Output 3. Input

Ordering Information

Product Number	Package	Packing Method	Operating Temperature
LM317T	TO-220 (Single Gauge)	Rail	0°C to +125°C
KA317TU	TO-220 (Dual Gauge)	Rail	0°C to +125°C

Block Diagram

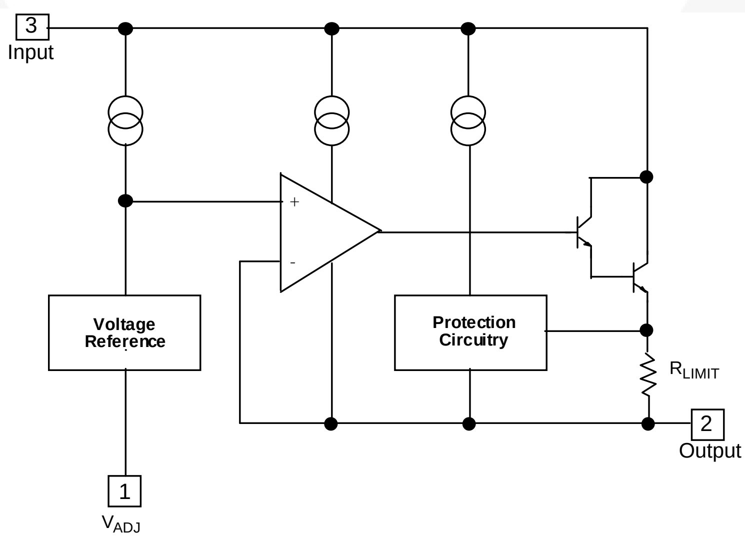

Figure 1. Block Diagram

Absolute Maximum Ratings

Stresses exceeding the absolute maximum ratings may damage the device. The device may not function or be operable above the recommended operating conditions and stressing the parts to these levels is not recommended. In addition, extended exposure to stresses above the recommended operating conditions may affect device reliability. The absolute maximum ratings are stress ratings only. Values are at T_A = 25°C unless otherwise noted.

Symbol	Parameter	Value	Unit
$V_I - V_O$	Input-Output Voltage Differential	40	V
T_{LEAD}	Lead Temperature	230	°C
T_J	Operating Junction Temperature Range	0 to +125	°C
T_{STG}	Storage Temperature Range	-65 to +125	°C
$\Delta V_O/\Delta T$	Temperature Coefficient of Output Voltage	±0.02	%/°C

Thermal Characteristics

Values are at T_A = 25°C unless otherwise noted.

Symbol	Parameter	Value	Units
P_D	Power Dissipation	Internally Limited	W
$R_{\theta JA}$	Thermal Resistance, Junction to Ambient	80	°C/W
$R_{\theta JC}$	Thermal Resistance, Junction to Case	5	°C/W

Electrical Characteristics

V_I-V_O = 5 V, I_O = 0.5 A, 0°C ≤ T_J ≤ +125°C, I_{MAX} = 1.5 A, P_{DMAX} = 20 W, unless otherwise specified.

Symbol	Parameter	Conditions		Min.	Typ.	Max.	Unit
R_{LINE}	Line Regulation[1]	T_A = +25°C, 3 V ≤ V_I - V_O ≤ 40 V			0.01	0.04	%/ V
		3 V ≤ V_I - V_O ≤ 40 V			0.02	0.07	
R_{LOAD}	Load Regulation[1]	T_A = +25°C, 10mA ≤ I_O ≤ I_{MAX}	V_O < 5 V		18	25	mV
			V_O ≥ 5 V		0.4	0.5	%/V_O
		10 mA ≤ I_O ≤ I_{MAX}	V_O < 5 V		40	70	mV
			V_O ≥ 5 V		0.8	1.5	%/V_O
I_{ADJ}	Adjustable Pin Current				46	100	µA
ΔI_{ADJ}	Adjustable Pin Current Change	3 V ≤ V_I - V_O ≤ 40 V, 10 mA ≤ I_O ≤ I_{MAX}, P_D ≤ P_{MAX}			2.0	5.0	µA
V_{REF}	Reference Voltage	3 V ≤ V_{IN} - V_O ≤ 40 V, 10 mA ≤ I_O ≤ I_{MAX}, P_D ≤ P_{MAX}		1.20	1.25	1.30	V
ST_T	Temperature Stability				0.7		%/V_O
$I_{L(MIN)}$	Minimum Load Current to Maintain Regulation	V_I - V_O = 40 V			3.5	12.0	mA
$I_{O(MAX)}$	Maximum Output Current	T_A = 25°C	V_I - V_O ≤ 15 V, P_D ≤ P_{MAX}	1.5	2.2		A
			V_I - V_O ≤ 40 V, P_D ≤ P_{MAX}		0.3		
e_N	RMS Noise,% of V_{OUT}	T_A = +25°C, 10 Hz ≤ f ≤ 10 kHz			0.003	0.010	%/V_O
RR	Ripple Rejection[2]	V_O = 10 V, f = 120 Hz	without C_{ADJ}		60		dB
			C_{ADJ} = 10 µF	66	75		
ST	Long-Term Stability, T_J = T_{HIGH}	T_A = +25°C for End Point Measurements, 1000 HR			0.3	1.0	%

Notes:
1. Load and line regulation are specified at constant junction temperature. Change in V_D due to heating effects must be taken into account separately. Pulse testing with low duty is used (P_{MAX} = 20 W).
2. C_{ADJ}, when used, is connected between the adjustment pin and ground.

Typical Performance Characteristics

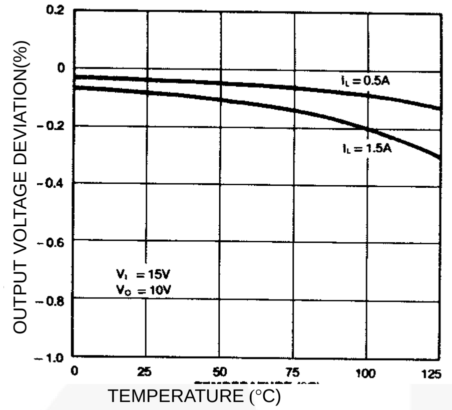

Figure 2. Load Regulation

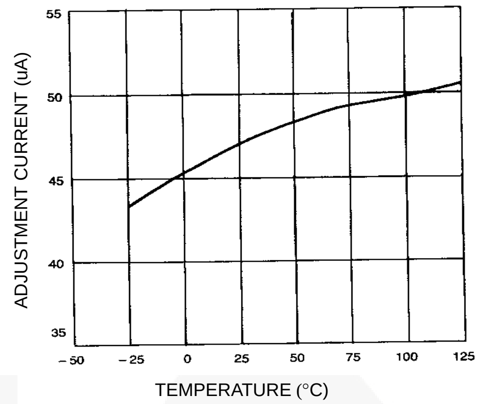

Figure 3. Adjustment Current

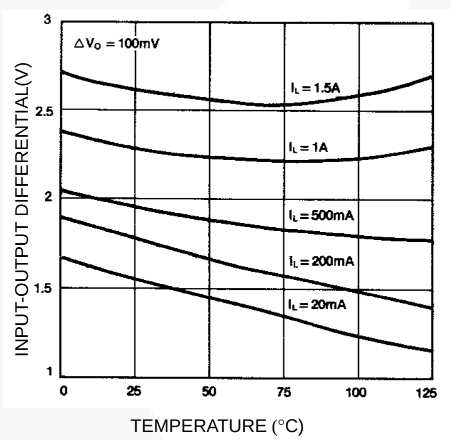

Figure 4. Dropout Voltage

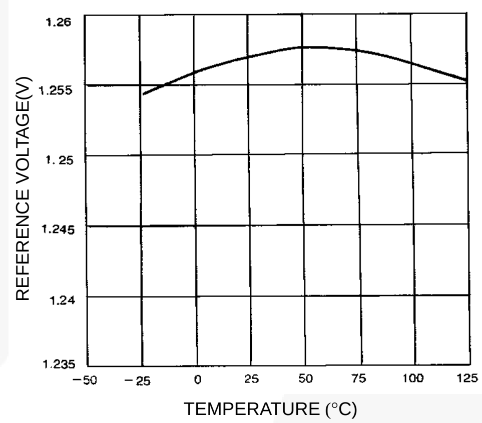

Figure 5. Reference Voltage

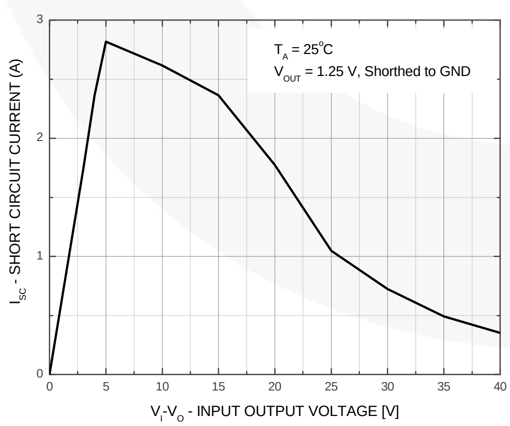

Figure 6. Short Circuit vs. Input-Output Voltage

Typical Application[3]

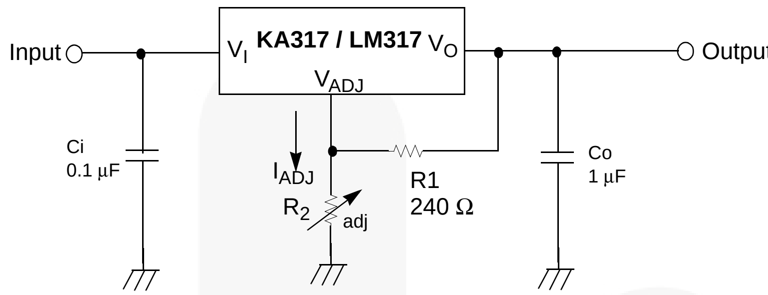

$$V_O = 1.25\text{ V}\,(1 + R_2 / R_1) + I_{ADJ}R_2$$

Figure 7. Typical Application

Note:

3. C_I is required when the regulator is located an appreciable distance from power supply filter. C_O is not needed for stability; however, it does improve transient response. Since I_{ADJ} is controlled to less than 100 µA, the error associated with this term is negligible in most applications.

Physical Dimensions

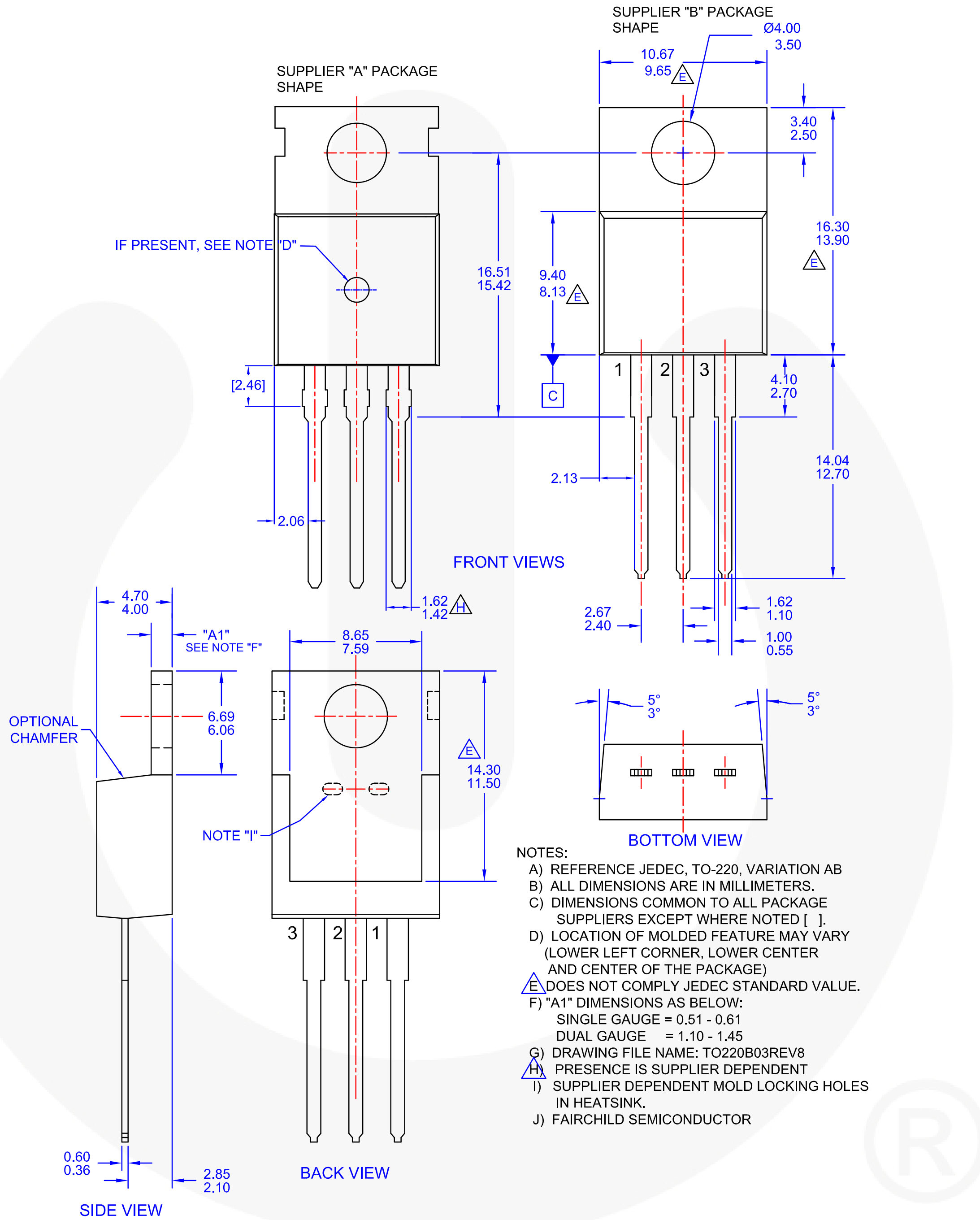

Figure 8. TO-220, MOLDED, 3LEAD, JEDEC VARIATION AB

TRADEMARKS

The following includes registered and unregistered trademarks and service marks, owned by Fairchild Semiconductor and/or its global subsidiaries, and is not intended to be an exhaustive list of all such trademarks.

AccuPower™
Awinda®
AX-CAP®*
BitSiC™
Build it Now™
CorePLUS™
CorePOWER™
CROSSVOLT™
CTL™
Current Transfer Logic™
DEUXPEED®
Dual Cool™
EcoSPARK®
EfficientMax™
ESBC™
®
Fairchild®
Fairchild Semiconductor®
FACT Quiet Series™
FACT®
FAST®
FastvCore™
FETBench™
FPS™
F-PFS™
FRFET®
Global Power Resource℠
GreenBridge™
Green FPS™
Green FPS™ e-Series™
G*max*™
GTO™
IntelliMAX™
ISOPLANAR™
Making Small Speakers Sound Louder and Better™
MegaBuck™
MICROCOUPLER™
MicroFET™
MicroPak™
MicroPak2™
MillerDrive™
MotionMax™
MotionGrid®
MTi®
MTx®
MVN®
mWSaver®
OptoHiT™
®
PowerTrench®
PowerXS™
Programmable Active Droop™
QFET®
QS™
Quiet Series™
RapidConfigure™
™
Saving our world, 1mW/W/kW at a time™
SignalWise™
SmartMax™
SMART START™
Solutions for Your Success™
SPM®
STEALTH™
SuperFET®
SuperSOT™-3
SuperSOT™-6
SuperSOT™-8
SupreMOS®
SyncFET™
Sync-Lock™
SYSTEM GENERAL®*
TinyBoost®
TinyBuck®
TinyCalc™
TinyLogic®
TINYOPTO™
TinyPower™
TinyPWM™
TinyWire™
TranSiC™
TriFault Detect™
TRUECURRENT®*
μSerDes™
SerDes™
UHC®
Ultra FRFET™
UniFET™
VCX™
VisualMax™
VoltagePlus™
XS™
Xsens™
仙童™

* Trademarks of System General Corporation, used under license by Fairchild Semiconductor.

DISCLAIMER

FAIRCHILD SEMICONDUCTOR RESERVES THE RIGHT TO MAKE CHANGES WITHOUT FURTHER NOTICE TO ANY PRODUCTS HEREIN TO IMPROVE RELIABILITY, FUNCTION, OR DESIGN. TO OBTAIN THE LATEST, MOST UP-TO-DATE DATASHEET AND PRODUCT INFORMATION, VISIT OUR WEBSITE AT HTTP://WWW.FAIRCHILDSEMI.COM. FAIRCHILD DOES NOT ASSUME ANY LIABILITY ARISING OUT OF THE APPLICATION OR USE OF ANY PRODUCT OR CIRCUIT DESCRIBED HEREIN; NEITHER DOES IT CONVEY ANY LICENSE UNDER ITS PATENT RIGHTS, NOR THE RIGHTS OF OTHERS. THESE SPECIFICATIONS DO NOT EXPAND THE TERMS OF FAIRCHILD'S WORLDWIDE TERMS AND CONDITIONS, SPECIFICALLY THE WARRANTY THEREIN, WHICH COVERS THESE PRODUCTS.

LIFE SUPPORT POLICY

FAIRCHILD'S PRODUCTS ARE NOT AUTHORIZED FOR USE AS CRITICAL COMPONENTS IN LIFE SUPPORT DEVICES OR SYSTEMS WITHOUT THE EXPRESS WRITTEN APPROVAL OF FAIRCHILD SEMICONDUCTOR CORPORATION.

As used herein:

1. Life support devices or systems are devices or systems which, (a) are intended for surgical implant into the body or (b) support or sustain life, and (c) whose failure to perform when properly used in accordance with instructions for use provided in the labeling, can be reasonably expected to result in a significant injury of the user.
2. A critical component in any component of a life support, device, or system whose failure to perform can be reasonably expected to cause the failure of the life support device or system, or to affect its safety or effectiveness.

ANTI-COUNTERFEITING POLICY

Fairchild Semiconductor Corporation's Anti-Counterfeiting Policy. Fairchild's Anti-Counterfeiting Policy is also stated on our external website, www.fairchildsemi.com, under Sales Support.

Counterfeiting of semiconductor parts is a growing problem in the industry. All manufacturers of semiconductor products are experiencing counterfeiting of their parts. Customers who inadvertently purchase counterfeit parts experience many problems such as loss of brand reputation, substandard performance, failed applications, and increased cost of production and manufacturing delays. Fairchild is taking strong measures to protect ourselves and our customers from the proliferation of counterfeit parts. Fairchild strongly encourages customers to purchase Fairchild parts either directly from Fairchild or from Authorized Fairchild Distributors who are listed by country on our web page cited above. Products customers buy either from Fairchild directly or from Authorized Fairchild Distributors are genuine parts, have full traceability, meet Fairchild's quality standards for handling and storage and provide access to Fairchild's full range of up-to-date technical and product information. Fairchild and our Authorized Distributors will stand behind all warranties and will appropriately address any warranty issues that may arise. Fairchild will not provide any warranty coverage or other assistance for parts bought from Unauthorized Sources. Fairchild is committed to combat this global problem and encourage our customers to do their part in stopping this practice by buying direct or from authorized distributors.

PRODUCT STATUS DEFINITIONS

Definition of Terms

Datasheet Identification	Product Status	Definition
Advance Information	Formative / In Design	Datasheet contains the design specifications for product development. Specifications may change in any manner without notice.
Preliminary	First Production	Datasheet contains preliminary data; supplementary data will be published at a later date. Fairchild Semiconductor reserves the right to make changes at any time without notice to improve design.
No Identification Needed	Full Production	Datasheet contains final specifications. Fairchild Semiconductor reserves the right to make changes at any time without notice to improve the design.
Obsolete	Not In Production	Datasheet contains specifications on a product that is discontinued by Fairchild Semiconductor. The datasheet is for reference information only.

Rev. I71

Single Supply, Rail-to-Rail Low Power FET-Input Op Amp

AD822

FEATURES
TRUE SINGLE SUPPLY OPERATION
- Output Swings Rail to Rail
- Input Voltage Range Extends Below Ground
- Single Supply Capability from +3 V to +36 V
- Dual Supply Capability from ±1.5 V to ±18 V

HIGH LOAD DRIVE
- Capacitive Load Drive of 350 pF, G = 1
- Minimum Output Current of 15 mA

EXCELLENT AC PERFORMANCE FOR LOW POWER
- 800 μA Max Quiescent Current per Amplifier
- Unity Gain Bandwidth: 1.8 MHz
- Slew Rate of 3.0 V/μs

GOOD DC PERFORMANCE
- 800 μV Max Input Offset Voltage
- 2 μV/°C Typ Offset Voltage Drift
- 25 pA Max Input Bias Current

LOW NOISE
- 13 nV/√Hz @ 10 kHz

NO PHASE INVERSION

APPLICATIONS
- Battery Powered Precision Instrumentation
- Photodiode Preamps
- Active Filters
- 12- to 14-Bit Data Acquisition Systems
- Medical Instrumentation
- Low Power References and Regulators

CONNECTION DIAGRAM
8-Pin Plastic DIP, Cerdip and SOIC

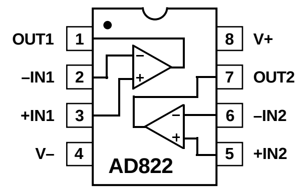

PRODUCT DESCRIPTION

The AD822 is a dual precision, low power FET input op amp that can operate from a single supply of +3.0 V to 36 V, or dual supplies of ±1.5 V to ±18 V. It has true single supply capability with an input voltage range extending below the negative rail, allowing the AD822 to accommodate input signals below ground in the single supply mode. Output voltage swing extends to within 10 mV of each rail providing the maximum output dynamic range.

Offset voltage of 800 μV max, offset voltage drift of 2 μV/°C, input bias currents below 25 pA and low input voltage noise provide dc precision with source impedances up to a Gigaohm. 1.8 MHz unity gain bandwidth, –93 dB THD at 10 kHz and 3 V/μs slew rate are provided with a low supply current of 800 μA per amplifier. The AD822 drives up to 350 pF of direct capacitive load as a follower, and provides a minimum output current of 15 mA. This allows the amplifier to handle a wide range of load conditions. This combination of ac and dc performance, plus the outstanding load drive capability, results in an exceptionally versatile amplifier for the single supply user.

The AD822 is available in four performance grades. The A and B grades are rated over the industrial temperature range of –40°C to +85°C. There is also a 3 volt grade—the AD822A-3V, rated over the industrial temperature range. The mil grade is rated over the military temperature range of –55°C to +125°C and is available processed on standard military drawing.

The AD822 is offered in three varieties of 8-pin package: plastic DIP, hermetic cerdip and surface mount (SOIC) as well as die form.

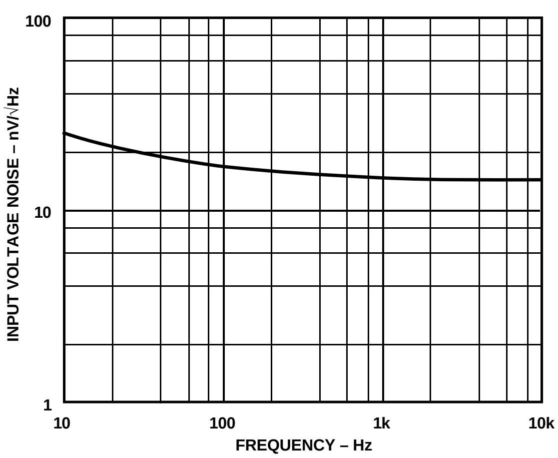

Input Voltage Noise vs. Frequency

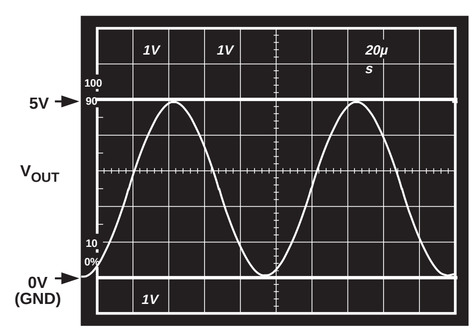

Gain of +2 Amplifier; V_S = +5, 0, V_{IN} = 2.5 V Sine Centered at 1.25 Volts, R_L = 100 kΩ

REV. A

One Technology Way, P.O. Box 9106, Norwood, MA 02062-9106, U.S.A.
Tel: 617/329-4700 Fax: 617/326-8703

AD822–SPECIFICATIONS (V_S = 0, 5 volts @ T_A = +25°C, V_{CM} = 0 V, V_{OUT} = 0.2 V unless otherwise noted)

Parameter	Conditions	AD822A Min	AD822A Typ	AD822A Max	AD822B Min	AD822B Typ	AD822B Max	AD822S[1] Min	AD822S[1] Typ	AD822S[1] Max	Units
DC PERFORMANCE											
Initial Offset			0.1	0.8		0.1	0.4		0.1	0.8	mV
Max Offset over Temperature			0.5	1.2		0.5	0.9		0.5		mV
Offset Drift			2			2			2		μV/°C
Input Bias Current	V_{CM} = 0 V to 4 V		2	25		2	10		2	25	pA
at T_{MAX}			0.5	5		0.5	2.5		0.5		nA
Input Offset Current			2	20		2	10		2	20	pA
at T_{MAX}			0.5			0.5			1.5		nA
Open-Loop Gain	V_O = 0.2 V to 4 V										
	R_L = 100 k	500	1000		500	1000		500	1000		V/mV
T_{MIN} to T_{MAX}		400			400						V/mV
	R_L = 10 k	80	150		80	150		80	150		V/mV
T_{MIN} to T_{MAX}		80			80						V/mV
	R_L = 1 k	15	30		15	30		15	30		V/mV
T_{MIN} to T_{MAX}		10			10						V/mV
NOISE/HARMONIC PERFORMANCE											
Input Voltage Noise											
0.1 Hz to 10 Hz			2			2			2		μV p-p
f = 10 Hz			25			25			25		$nV/\sqrt{Hz}$
f = 100 Hz			21			21			21		$nV/\sqrt{Hz}$
f = 1 kHz			16			16			16		$nV/\sqrt{Hz}$
f = 10 kHz			13			13			13		$nV/\sqrt{Hz}$
Input Current Noise											
0.1 Hz to 10 Hz			18			18			18		fA p-p
f = 1 kHz			0.8			0.8			0.8		$fA/\sqrt{Hz}$
Harmonic Distortion	R_L = 10 k to 2.5 V										
f = 10 kHz	V_O = 0.25 V to 4.75 V		–93			–93			–93		dB
DYNAMIC PERFORMANCE											
Unity Gain Frequency			1.8			1.8			1.8		MHz
Full Power Response	V_O p-p = 4.5 V		210			210			210		kHz
Slew Rate			3			3			3		V/μs
Settling Time											
to 0.1%	V_O = 0.2 V to 4.5 V		1.4			1.4			1.4		μs
to 0.01%			1.8			1.8			1.8		μs
MATCHING CHARACTERISTICS											
Initial Offset				1.0			0.5			1.6	mV
Max Offset Over Temperature				1.6			1.3				mV
Offset Drift			3			3					μV/°C
Input Bias Current				20			10			20	pA
Crosstalk @ f = 1 kHz	R_L = 5 kΩ		–130			–130			–130		dB
f = 100 kHz			–93			–93			–93		dB
INPUT CHARACTERISTICS											
Common-Mode Voltage Range[2]		–0.2		4	–0.2		4	–0.2		4	V
T_{MIN} to T_{MAX}		–0.2		4	–0.2		4				V
CMRR	V_{CM} = 0 V to +2 V	66	80		69	80		66	80		dB
T_{MIN} to T_{MAX}		66			66						dB
Input Impedance											
Differential			10^{13}‖0.5			10^{13}‖0.5			10^{13}‖0.5		Ω‖pF
Common Mode			10^{13}‖2.8			10^{13}‖2.8			10^{13}‖2.8		Ω‖pF
OUTPUT CHARACTERISTICS											
Output Saturation Voltage[3]											
$V_{OL}–V_{EE}$	I_{SINK} = 20 μA		5	7		5	7		5	7	mV
T_{MIN} to T_{MAX}				10			10				mV
$V_{CC}–V_{OH}$	I_{SOURCE} = 20 μA		10	14		10	14		10	14	mV
T_{MIN} to T_{MAX}				20			20				mV
$V_{OL}–V_{EE}$	I_{SINK} = 2 mA		40	55		40	55		40	55	mV
T_{MIN} to T_{MAX}				80			80				mV
$V_{CC}–V_{OH}$	I_{SOURCE} = 2 mA		80	110		80	110		80	110	mV
T_{MIN} to T_{MAX}				160			160				mV
$V_{OL}–V_{EE}$	I_{SINK} = 15 mA		300	500		300	500		300	500	mV
T_{MIN} to T_{MAX}				1000			1000				mV
$V_{CC}–V_{OH}$	I_{SOURCE} = 15 mA		800	1500		800	1500		800	1500	mV
T_{MIN} to T_{MAX}				1900			1900				mV
Operating Output Current		15			15			15			mA
T_{MIN} to T_{MAX}		12			12						mA
Capacitive Load Drive			350			350			350		pF
POWER SUPPLY											
Quiescent Current T_{MIN} to T_{MAX}			1.24	1.6		1.24	1.6		1.24		mA
Power Supply Rejection	V_S+ = 5 V to 15 V	70	80		66	80		70	80		dB
T_{MIN} to T_{MAX}		70			66						dB

(V_S = ±5 volts @ T_A = +25°C, V_{CM} = 0 V, V_{OUT} = 0 V unless otherwise noted)

Parameter	Conditions	AD822A Min	AD822A Typ	AD822A Max	AD822B Min	AD822B Typ	AD822B Max	AD822S[1] Min	AD822S[1] Typ	AD822S[1] Max	Units
DC PERFORMANCE											
Initial Offset			0.1	0.8		0.1	0.4		0.1		mV
Max Offset over Temperature			0.5	1.5		0.5	1		0.5		mV
Offset Drift			2			2			2		µV/°C
Input Bias Current	V_{CM} = –5 V to 4 V		2	25		2	10		2	25	pA
at T_{MAX}			0.5	5		0.5	2.5		0.5		nA
Input Offset Current			2	20		2	10		2		pA
at T_{MAX}			0.5			0.5			1.5		nA
Open-Loop Gain	V_O = –4 V to 4 V										
	R_L = 100 k	400	1000		400	1000		400	1000		V/mV
T_{MIN} to T_{MAX}		400			400						V/mV
	R_L = 10 k	80	150		80	150		80	150		V/mV
T_{MIN} to T_{MAX}		80			80						V/mV
	R_L = 1 k	20	30		20	30		20	30		V/mV
T_{MIN} to T_{MAX}		10			10						V/mV
NOISE/HARMONIC PERFORMANCE											
Input Voltage Noise											
0.1 Hz to 10 Hz			2			2			2		µV p-p
f = 10 Hz			25			25			25		$nV/\sqrt{Hz}$
f = 100 Hz			21			21			21		$nV/\sqrt{Hz}$
f = 1 kHz			16			16			16		$nV/\sqrt{Hz}$
f = 10 kHz			13			13			13		$nV/\sqrt{Hz}$
Input Current Noise											
0.1 Hz to 10 Hz			18			18			18		fA p-p
f = 1 kHz			0.8			0.8			0.8		$fA/\sqrt{Hz}$
Harmonic Distortion	R_L = 10 k										
f = 10 kHz	V_O = ±4.5 V		–93			–93			–93		dB
DYNAMIC PERFORMANCE											
Unity Gain Frequency			1.9			1.9			1.9		MHz
Full Power Response	V_O p-p = 9 V		105			105			105		kHz
Slew Rate			3			3			3		V/µs
Settling Time											
to 0.1%	V_O = 0 V to ±4.5 V		1.4			1.4			1.4		µs
to 0.01%			1.8			1.8			1.8		µs
MATCHING CHARACTERISTICS											
Initial Offset				1.0			0.5			1.6	mV
Max Offset Over Temperature				3			2			2	mV
Offset Drift			3			3					µV/°C
Input Bias Current				25			10			25	pA
Crosstalk @ f = 1 kHz	R_L = 5 kΩ		–130			–130			–130		dB
f = 100 kHz			–93			–93			–93		dB
INPUT CHARACTERISTICS											
Common-Mode Voltage Range[2]		–5.2		4	–5.2		4	–5.2		4	V
T_{MIN} to T_{MAX}		–5.2		4	–5.2		4				V
CMRR	V_{CM} = –5 V to +2 V	66	80		69	80		66	80		dB
T_{MIN} to T_{MAX}		66			66						dB
Input Impedance											
Differential			10^{13}‖0.5			10^{13}‖0.5			10^{13}‖0.5		Ω‖pF
Common Mode			10^{13}‖2.8			10^{13}‖2.8			10^{13}‖2.8		Ω‖pF
OUTPUT CHARACTERISTICS											
Output Saturation Voltage[3]											
V_{OL}–V_{EE}	I_{SINK} = 20 µA		5	7		5	7		5	7	mV
T_{MIN} to T_{MAX}				10			10				mV
V_{CC}–V_{OH}	I_{SOURCE} = 20 µA		10	14		10	14		10	14	mV
T_{MIN} to T_{MAX}				20			20				mV
V_{OL}–V_{EE}	I_{SINK} = 2 mA		40	55		40	55		40	55	mV
T_{MIN} to T_{MAX}				80			80				mV
V_{CC}–V_{OH}	I_{SOURCE} = 2 mA		80	110		80	110		80	110	mV
T_{MIN} to T_{MAX}				160			160				mV
V_{OL}–V_{EE}	I_{SINK} = 15 mA		300	500		300	500		300	500	mV
T_{MIN} to T_{MAX}				1000			1000				mV
V_{CC}–V_{OH}	I_{SOURCE} = 15 mA		800	1500		800	1500		800	1500	mV
T_{MIN} to T_{MAX}				1900			1900				mV
Operating Output Current		15			15			15			mA
T_{MIN} to T_{MAX}		12			12						mA
Capacitive Load Drive			350			350			350		pF
POWER SUPPLY											
Quiescent Current T_{MIN} to T_{MAX}			1.3	1.6		1.3	1.6		1.3		mA
Power Supply Rejection	V_S+ = 5 V to 15 V	70	80		66	80		70	80		dB
T_{MIN} to T_{MAX}		70			66						dB

AD822–SPECIFICATIONS (V_S = ±15 volts @ T_A = +25°C, V_{CM} = 0 V, V_{OUT} = 0 V unless otherwise noted)

Parameter	Conditions	AD822A			AD822B			AD822S[1]			Units
		Min	Typ	Max	Min	Typ	Max	Min	Typ	Max	
DC PERFORMANCE											
Initial Offset			0.4	2		0.3	1.5		0.4	2.0	mV
Max Offset over Temperature			0.5	3		0.5	2.5		0.5		mV
Offset Drift			2			2			2		µV/°C
Input Bias Current	V_{CM} = 0 V		2	25		2	12		2	25	pA
	V_{CM} = –10 V		40			40			40		pA
at T_{MAX}	V_{CM} = 0 V		0.5	5		0.5	2.5		0.5		nA
Input Offset Current			2	20		2	12		2	20	pA
at T_{MAX}			0.5			0.5			1.5		nA
Open-Loop Gain	V_O = +10 V to –10 V										
	R_L = 100 k	500	2000		500	2000		500	2000		V/mV
T_{MIN} to T_{MAX}		500			500						V/mV
	R_L = 10 k	100	500		100	500		150	400		V/mV
T_{MIN} to T_{MAX}		100			100						V/mV
	R_L = 1 k	30	45		30	45		30	45		V/mV
T_{MIN} to T_{MAX}		20			20						V/mV
NOISE/HARMONIC PERFORMANCE											
Input Voltage Noise											
0.1 Hz to 10 Hz			2			2			2		µV p-p
f = 10 Hz			25			25			25		nV/√Hz
f = 100 Hz			21			21			21		nV/√Hz
f = 1 kHz			16			16			16		nV/√Hz
f = 10 kHz			13			13			13		nV/√Hz
Input Current Noise											
0.1 Hz to 10 Hz			18			18			18		fA p-p
f = 1 kHz			0.8			0.8			0.8		fA/√Hz
Harmonic Distortion	R_L = 10 k										
f = 10 kHz	V_O = ±10 V		–85			–85			–85		dB
DYNAMIC PERFORMANCE											
Unity Gain Frequency			1.9			1.9			1.9		MHz
Full Power Response	V_O p-p = 20 V		45			45			45		kHz
Slew Rate			3			3			3		V/µs
Settling Time											
to 0.1%	V_O = 0 V to ±10 V		4.1			4.1			4.1		µs
to 0.01%			4.5			4.5			4.5		µs
MATCHING CHARACTERISTICS											
Initial Offset				3			2			0.8	mV
Max Offset Over Temperature				4			2.5			1.0	mV
Offset Drift			3			3					µV/°C
Input Bias Current				25			12			25	pA
Crosstalk @ f = 1 kHz	R_L = 5 kΩ		–130			–130			–130		dB
f = 100 kHz			–93			–93			–93		dB
INPUT CHARACTERISTICS											
Common-Mode Voltage Range[2]		–15.2		14	–15.2		14	–15.2		14	V
T_{MIN} to T_{MAX}		–15.2		14	–15.2		14				V
CMRR	V_{CM} = –15 V to 12 V	70	80		74	90		70	90		dB
T_{MIN} to T_{MAX}		70			74						dB
Input Impedance											
Differential			10^{13}‖0.5			10^{13}‖0.5			10^{13}‖0.5		Ω‖pF
Common Mode			10^{13}‖2.8			10^{13}‖2.8			10^{13}‖2.8		Ω‖pF
OUTPUT CHARACTERISTICS											
Output Saturation Voltage[3]											
V_{OL}–V_{EE}	I_{SINK} = 20 µA		5	7		5	7		5	7	mV
T_{MIN} to T_{MAX}				10			10				mV
V_{CC}–V_{OH}	I_{SOURCE} = 20 µA		10	14		10	14		10	14	mV
T_{MIN} to T_{MAX}				20			20				mV
V_{OL}–V_{EE}	I_{SINK} = 2 mA		40	55		40	55		40	55	mV
T_{MIN} to T_{MAX}				80			80				mV
V_{CC}–V_{OH}	I_{SOURCE} = 2 mA		80	110		80	110		80	110	mV
T_{MIN} to T_{MAX}				160			160				mV
V_{OL}–V_{EE}	I_{SINK} = 15 mA		300	500		300	500		300	500	mV
T_{MIN} to T_{MAX}				1000			1000				mV
V_{CC}–V_{OH}	I_{SOURCE} = 15 mA		800	1500		800	1500		800	1500	mV
T_{MIN} to T_{MAX}				1900			1900				mV
Operating Output Current		20			20			20			mA
T_{MIN} to T_{MAX}		15			15						mA
Capacitive Load Drive			350			350			350		pF
POWER SUPPLY											
Quiescent Current T_{MIN} to T_{MAX}			1.4	1.8		1.4	1.8		1.4		mA
Power Supply Rejection	V_S+ = 5 V to 15 V	70	80		70	80		70	80		dB
T_{MIN} to T_{MAX}		70			70						dB

(V_S = 0, 3 volts @ T_A = +25°C, V_{CM} = 0 V, V_{OUT} = 0.2 V unless otherwise noted)

Parameter	Conditions	AD822A-3 V Min	Typ	Max	Units
DC PERFORMANCE					
Initial Offset			0.2	1	mV
Max Offset over Temperature			0.5	1.5	mV
Offset Drift			1		μV/°C
Input Bias Current	V_{CM} = 0 V to +2 V		2	25	pA
at T_{MAX}			0.5	5	nA
Input Offset Current			2	20	pA
at T_{MAX}			0.5		nA
Open-Loop Gain	V_O = 0.2 V to 2 V				
	R_L = 100 k	300	1000		V/mV
T_{MIN} to T_{MAX}		300			V/mV
	R_L = 10 k	60	150		V/mV
T_{MIN} to T_{MAX}		60			V/mV
	R_L = 1 k	10	30		V/mV
T_{MIN} to T_{MAX}		8			V/mV
NOISE/HARMONIC PERFORMANCE					
Input Voltage Noise					
0.1 Hz to 10 Hz			2		μV p-p
f = 10 Hz			25		nV/√Hz
f = 100 Hz			21		nV/√Hz
f = 1 kHz			16		nV/√Hz
f = 10 kHz			13		nV/√Hz
Input Current Noise					
0.1 Hz to 10 Hz			18		fA p-p
f = 1 kHz			0.8		fA/√Hz
Harmonic Distortion	R_L = 10 k to 1.5 V				
f = 10 kHz	V_O = ±1.25 V		–92		dB
DYNAMIC PERFORMANCE					
Unity Gain Frequency			1.5		MHz
Full Power Response	V_O p-p = 2.5 V		240		kHz
Slew Rate			3		V/μs
Settling Time					
to 0.1%	V_O = 0.2 V to 2.5 V		1		μs
to 0.01%			1.4		μs
MATCHING CHARACTERISTICS					
Initial Offset				1	mV
Max Offset Over Temperature				2	mV
Offset Drift			2		μV/°C
Input Bias Current				10	pA
Crosstalk @ f = 1 kHz	R_L = 5 kΩ		–130		dB
f = 100 kHz			–93		dB
INPUT CHARACTERISTICS					
Common-Mode Voltage Range[2]		–0.2		2	V
T_{MIN} to T_{MAX}		–0.2		2	V
CMRR	V_{CM} = 0 V to +1 V	60	74		dB
T_{MIN} to T_{MAX}		60			dB
Input Impedance					
Differential			10^{13}‖0.5		Ω‖pF
Common Mode			10^{13}‖2.8		Ω‖pF
OUTPUT CHARACTERISTICS					
Output Saturation Voltage[3]					
V_{OL}–V_{EE}	I_{SINK} = 20 μA		5	7	mV
T_{MIN} to T_{MAX}				10	mV
V_{CC}–V_{OH}	I_{SOURCE} = 20 μA		10	14	mV
T_{MIN} to T_{MAX}				20	mV
V_{OL}–V_{EE}	I_{SINK} = 2 mA		40	55	mV
T_{MIN} to T_{MAX}				80	mV
V_{CC}–V_{OH}	I_{SOURCE} = 2 mA		80	110	mV
T_{MIN} to T_{MAX}				160	mV
V_{OL}–V_{EE}	I_{SINK} = 10 mA		200	400	mV
T_{MIN} to T_{MAX}				400	mV
V_{CC}–V_{OH}	I_{SOURCE} = 10 mA		500	1000	mV
T_{MIN} to T_{MAX}				1000	mV
Operating Output Current		15			mA
T_{MIN} to T_{MAX}		12			mA
Capacitive Load Drive			350		pF
POWER SUPPLY					
Quiescent Current T_{MIN} to T_{MAX}			1.24	1.6	mA
Power Supply Rejection	V_S+ = 3 V to 15 V	70	80		dB
T_{MIN} to T_{MAX}		70			dB

NOTES
[1]See standard military drawing for 883B specifications.
[2]This is a functional specification. Amplifier bandwidth decreases when the input common-mode voltage is driven in the range ($+V_S$ – 1 V) to $+V_S$. Common-mode error voltage is typically less than 5 mV with the common-mode voltage set at 1 volt below the positive supply.
[3]V_{OL}–V_{EE} is defined as the difference between the lowest possible output voltage (V_{OL}) and the minus voltage supply rail (V_{EE}). V_{CC}–V_{OH} is defined as the difference between the highest possible output voltage (V_{OH}) and the positive supply voltage (V_{CC}).

Specifications subject to change without notice.

CAUTION

ESD (electrostatic discharge) sensitive device. Electrostatic charges as high as 4000 V readily accumulate on the human body and test equipment and can discharge without detection. Although the AD822 features proprietary ESD protection circuitry, permanent damage may occur on devices subjected to high energy electrostatic discharges. Therefore, proper ESD precautions are recommended to avoid performance degradation or loss of functionality.

ABSOLUTE MAXIMUM RATINGS[1]

Supply Voltage . . . . ±18 V
Internal Power Dissipation
  Plastic DIP (N) . . . . Observe Derating Curves
  Cerdip (Q) . . . . Observe Derating Curves
  SOIC (R) . . . . Observe Derating Curves
Input Voltage . . . . ($+V_S$ + 0.2 V) to –(20 V + V_S)
Output Short Circuit Duration . . . . Indefinite
Differential Input Voltage . . . . ±30 V
Storage Temperature Range (N) . . . . . . –65°C to +125°C
Storage Temperature Range (Q) . . . . . . –65°C to +150°C
Storage Temperature Range (R) . . . . . . –65°C to +150°C
Operating Temperature Range
  AD822A/B . . . . –40°C to +85°C
  AD822S . . . . –55°C to +125°C
Lead Temperature Range (Soldering 60 sec) . . . . . . +260°C

NOTES
[1]Stresses above those listed under "Absolute Maximum Ratings" may cause permanent damage to the device. This is a stress rating only and functional operation of the device at these or any other conditions above those indicated in the operational section of this specification is not implied. Exposure to absolute maximum rating conditions for extended periods may affect device reliability.
[2]8-Pin Plastic DIP Package: θ_{JA} = 90°C/Watt
8-Pin Cerdip Package: θ_{JA} = 110°C/Watt
8-Pin SOIC Package: θ_{JA} = 160°C/Watt

MAXIMUM POWER DISSIPATION

The maximum power that can be safely dissipated by the AD822 is limited by the associated rise in junction temperature. For plastic packages, the maximum safe junction temperature is 145°C. For the cerdip packages, the maximum junction temperature is 175°C. If these maximums are exceeded momentarily, proper circuit operation will be restored as soon as the die temperature is reduced. Leaving the device in the "overheated" condition for an extended period can result in device burnout. To ensure proper operation, it is important to observe the derating curves shown in Figure 24.

While the AD822 is internally short circuit protected, this may not be sufficient to guarantee that the maximum junction temperature is not exceeded under all conditions. With power supplies ±12 volts (or less) at an ambient temperature of +25°C or less, if the output node is shorted to a supply rail, then the amplifier will not be destroyed, even if this condition persists for an extended period.

ORDERING GUIDE

Model[1]	Temperature Range	Package Description	Package Option
AD822AN	–40°C to +85°C	8-Pin Plastic Mini-DIP	N-8
AD822BN	–40°C to +85°C	8-Pin Plastic Mini-DIP	N-8
AD822AR	–40°C to +85°C	8-Pin SOIC	R-8
AD822BR	–40°C to +85°C	8-Pin SOIC	R-8
AD822AR-3V	–40°C to +85°C	8-Pin SOIC	R-8
AD822AN-3V	–40°C to +85°C	8-Pin Plastic Mini-DIP	N-8
AD822A Chips	–40°C to +85°C	Die	
Standard Military Drawing[2]	–55°C to +125°C	8-Pin Cerdip	Q-8

NOTES
[1]Spice model is available on ADI Model Disc.
[2]Contact factory for availability.

METALIZATION PHOTOGRAPH

Contact factory for latest dimensions.
Dimensions shown in inches and (mm).

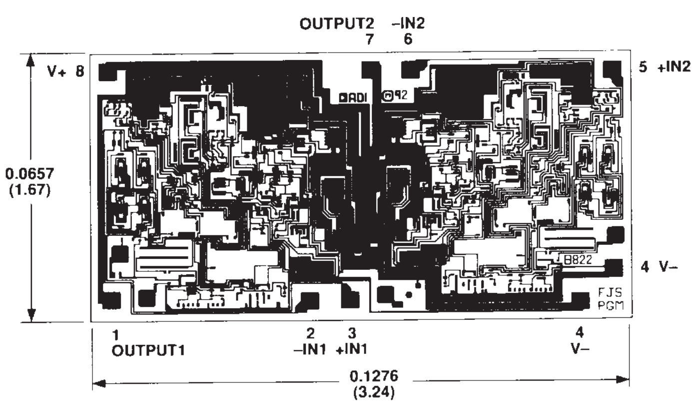

NOTE: BACK OF DIE IS AT $+V_S$ POTENTIAL.

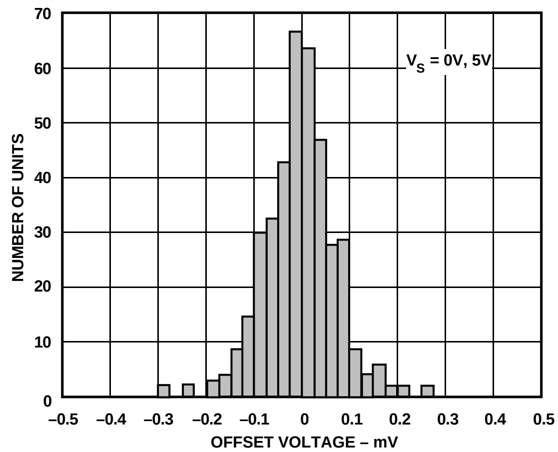

Figure 1. Typical Distribution of Offset Voltage (390 Units)

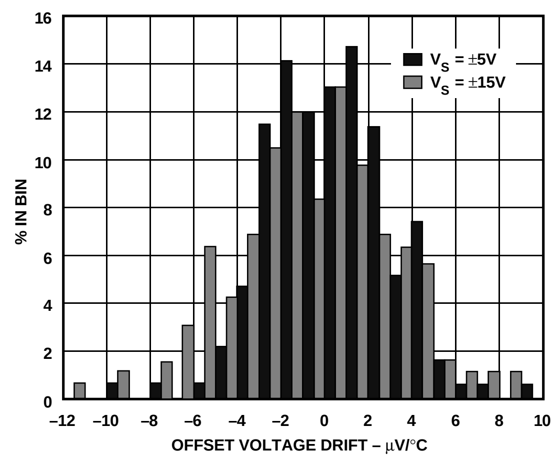

Figure 2. Typical Distribution of Offset Voltage Drift (100 Units)

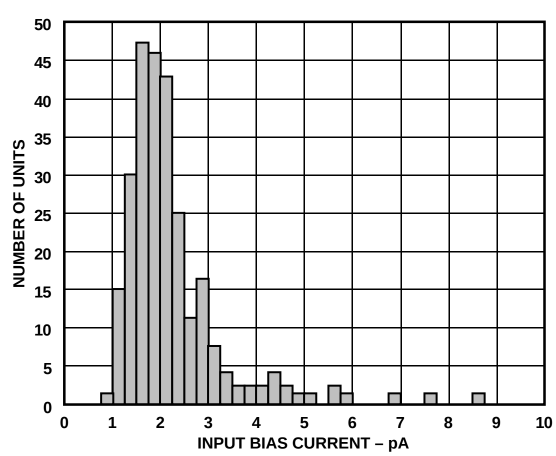

Figure 3. Typical Distribution of Input Bias Current (213 Units)

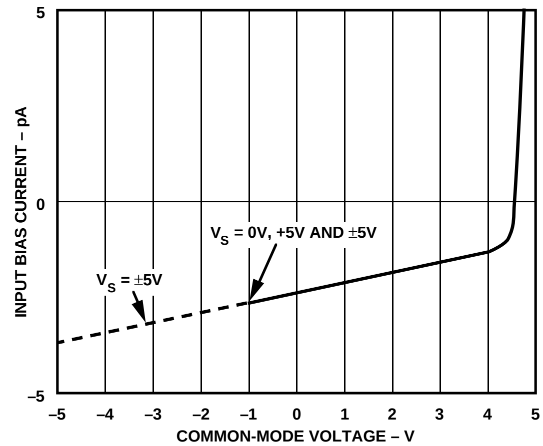

Figure 4. Input Bias Current vs. Common-Mode Voltage; V_S = +5 V, 0 V and V_S = ±5 V

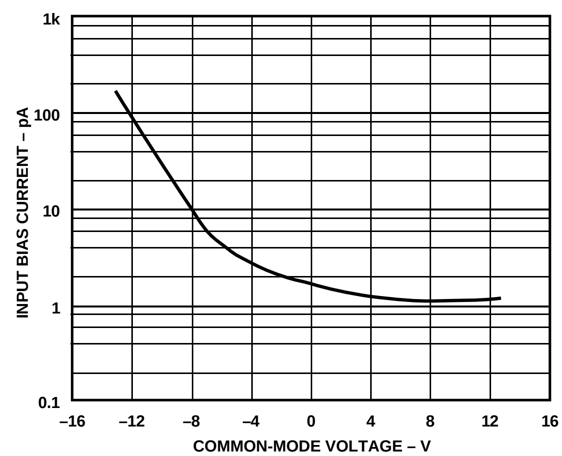

Figure 5. Input Bias Current vs. Common-Mode Voltage; V_S = ±15 V

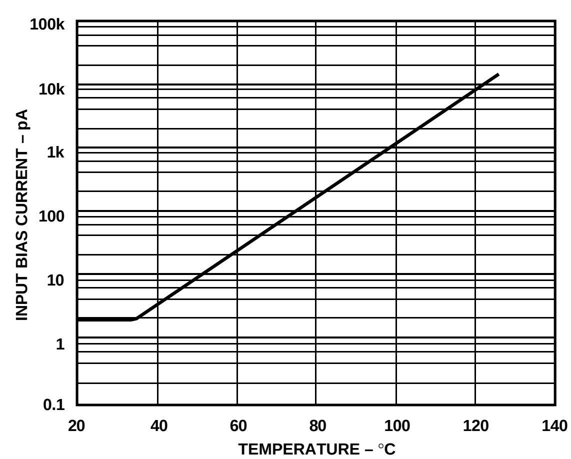

Figure 6. Input Bias Current vs. Temperature; V_S = 5 V, V_{CM} = 0

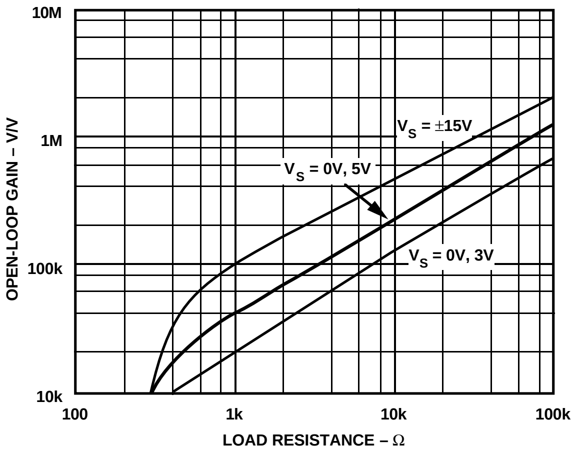

Figure 7. Open-Loop Gain vs. Load Resistance

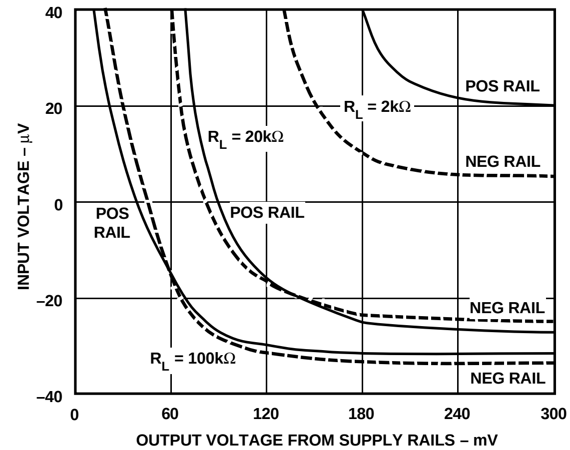

Figure 10. Input Error Voltage with Output Voltage within 300 mV of Either Supply Rail for Various Resistive Loads; $V_S = \pm 5$ V

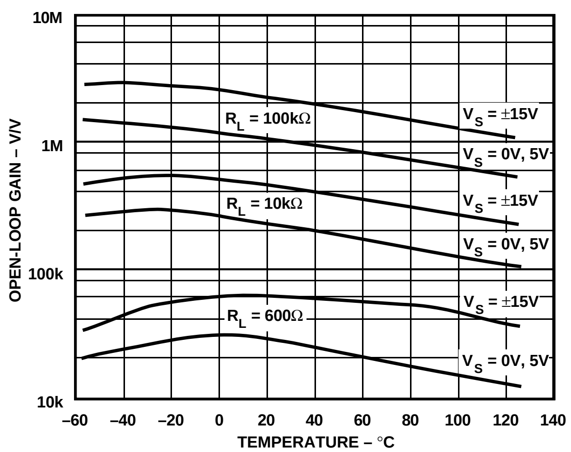

Figure 8. Open-Loop Gain vs. Temperature

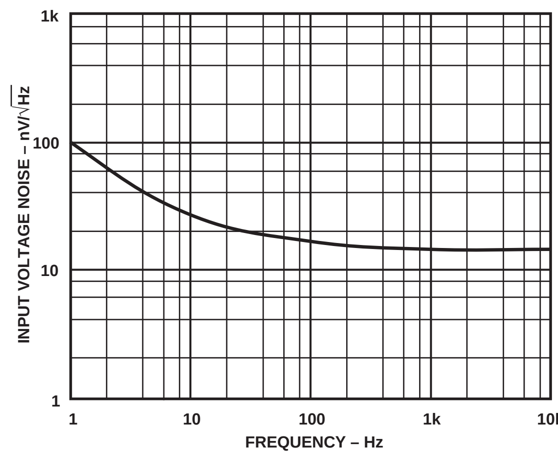

Figure 11. Input Voltage Noise vs. Frequency

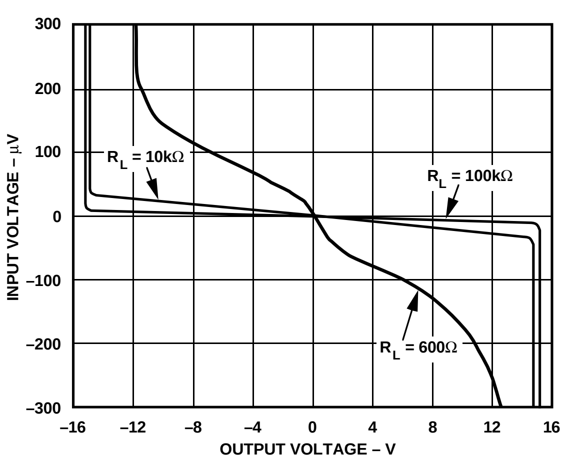

Figure 9. Input Error Voltage vs. Output Voltage for Resistive Loads

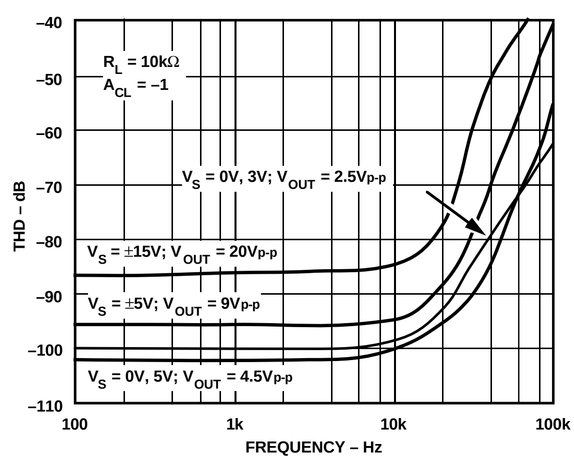

Figure 12. Total Harmonic Distortion vs. Frequency

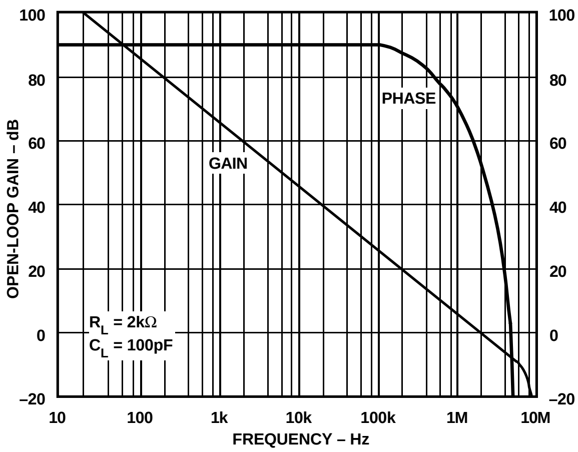

Figure 13. Open-Loop Gain and Phase Margin vs. Frequency

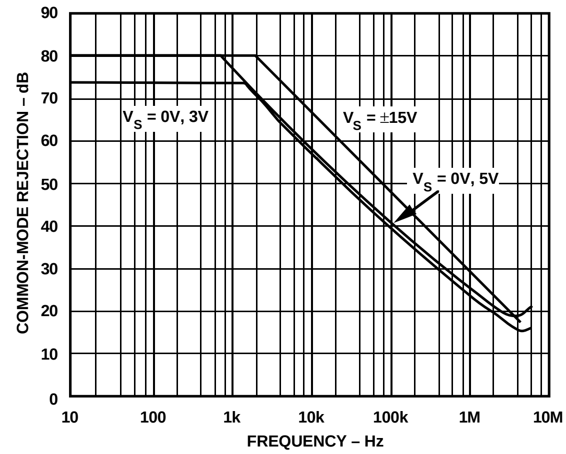

Figure 16. Common-Mode Rejection vs. Frequency

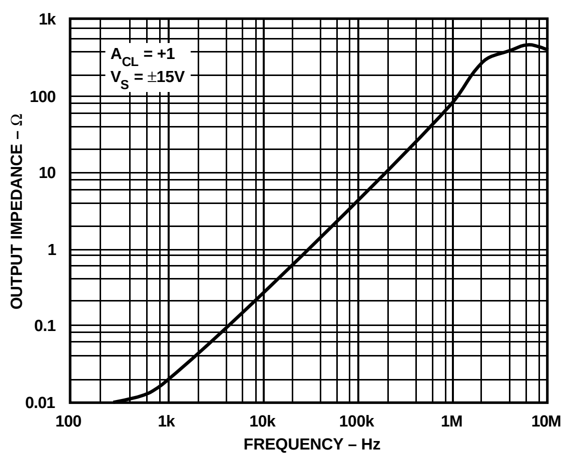

Figure 14. Output Impedance vs. Frequency

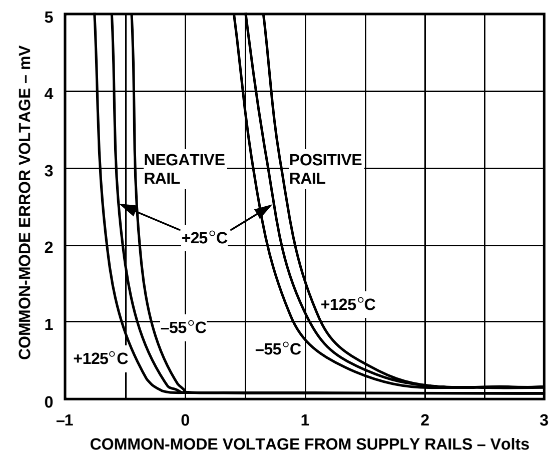

Figure 17. Absolute Common-Mode Error vs. Common-Mode Voltage from Supply Rails (V_S – V_{CM})

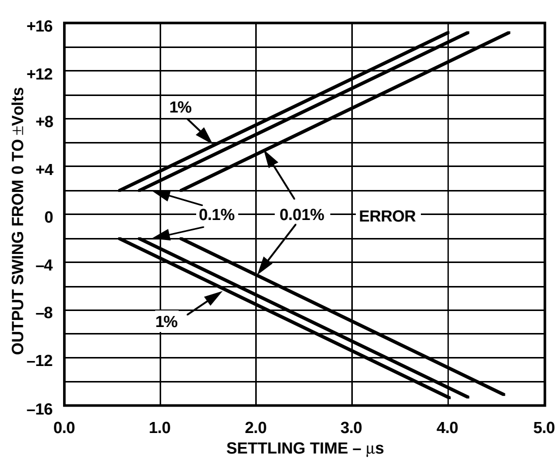

Figure 15. Output Swing and Error vs. Settling Time

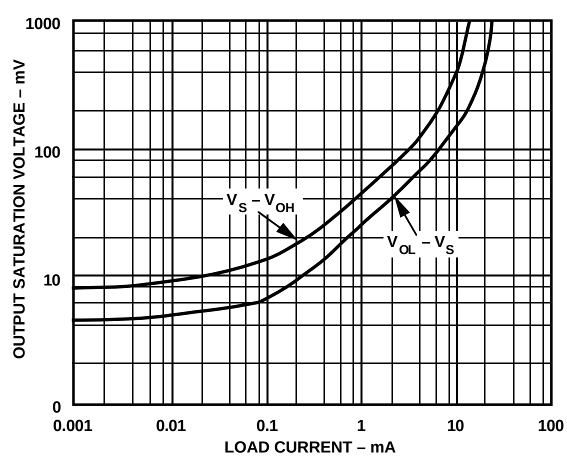

Figure 18. Output Saturation Voltage vs. Load Current

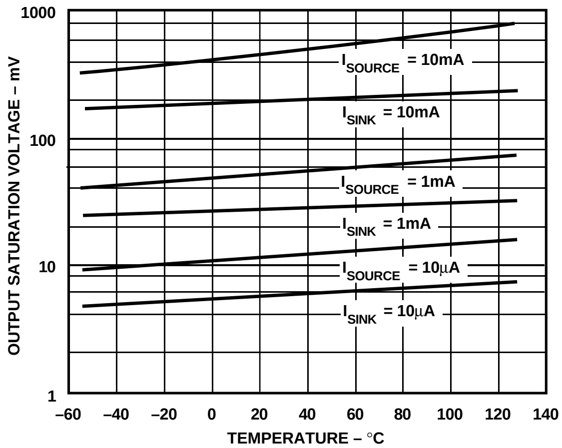

Figure 19. Output Saturation Voltage vs. Temperature

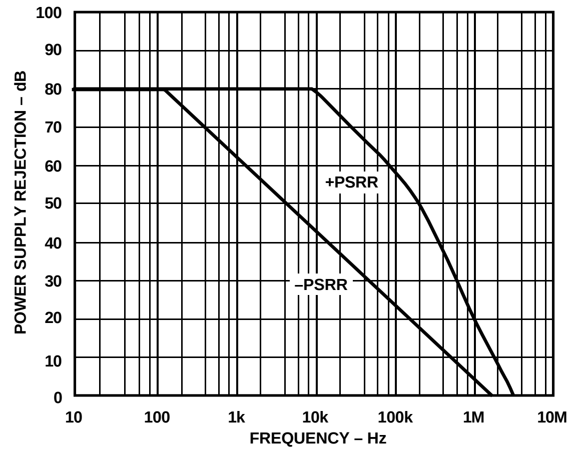

Figure 22. Power Supply Rejection vs. Frequency

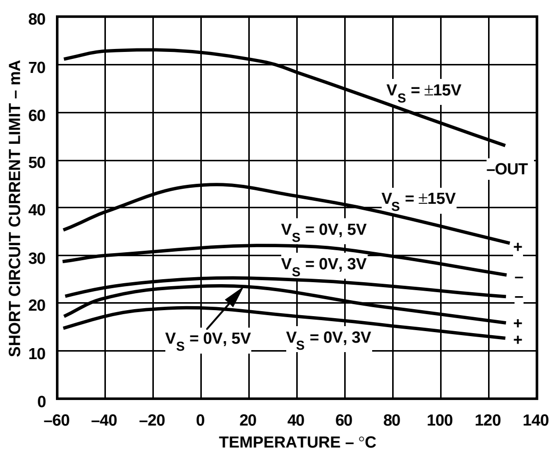

Figure 20. Short Circuit Current Limit vs. Temperature

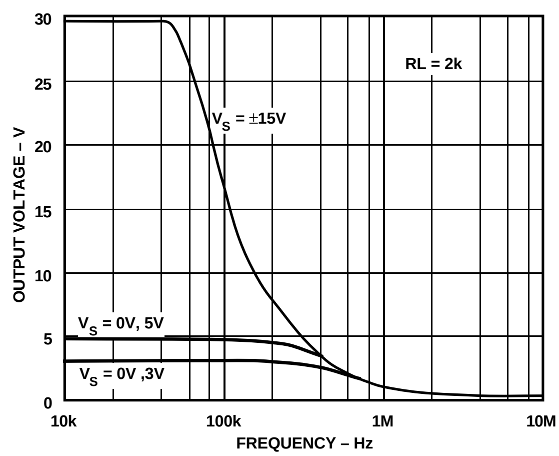

Figure 23. Large Signal Frequency Response

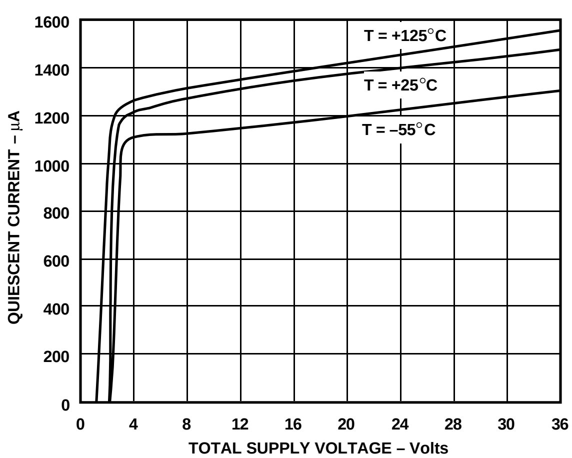

Figure 21. Quiescent Current vs. Supply Voltage vs. Temperature

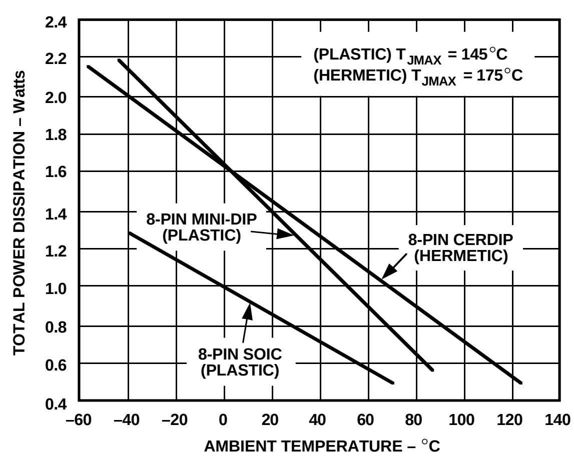

Figure 24. Maximum Power Dissipation vs. Temperature for Plastic and Hermetic Packages

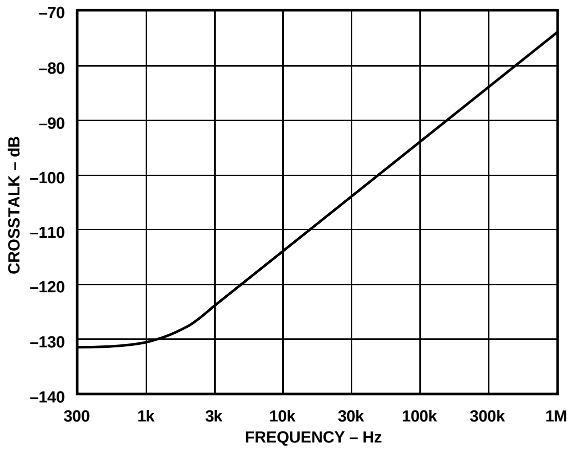

Figure 25. Crosstalk vs. Frequency

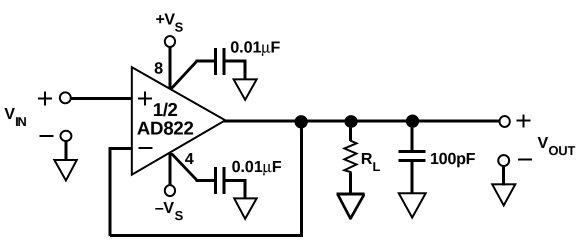

Figure 26. Unity-Gain Follower

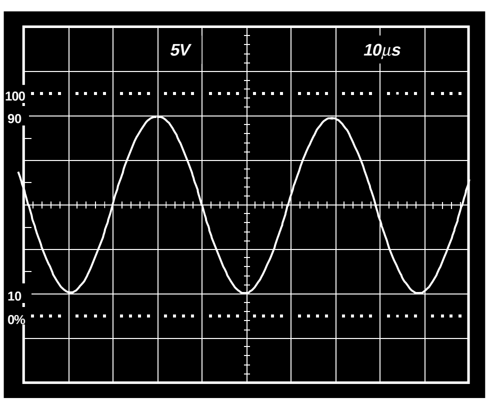

Figure 27. 20 V p-p, 25 kHz Sine Wave Input; Unity Gain Follower; R_L = 600 Ω, V_S = ±15 V

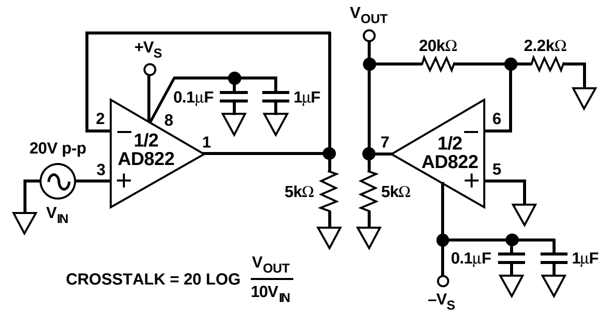

Figure 28. Crosstalk Test Circuit

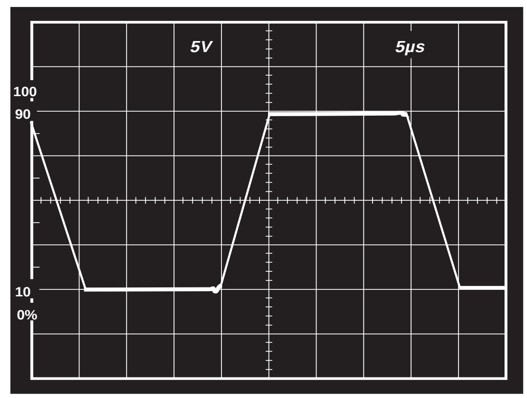

Figure 29. Large Signal Response Unity Gain Follower; V_S = ±15 V, R_L = 10 kΩ

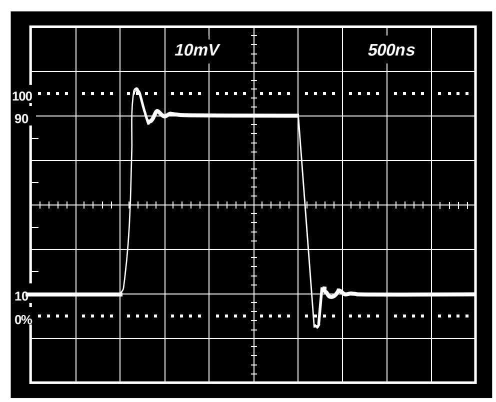

Figure 30. Small Signal Response Unity Gain Follower; V_S = ±15 V, R_L = 10 kΩ

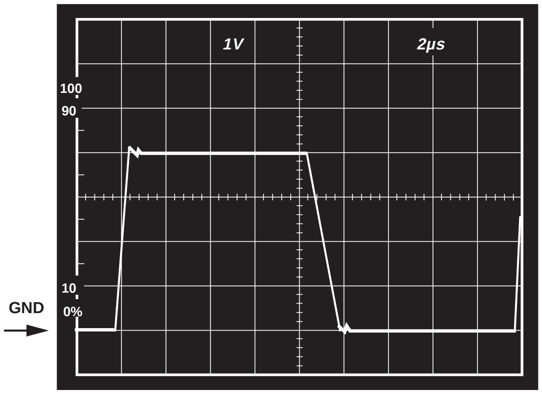

Figure 31. V_S = +5 V, 0 V; Unity Gain Follower Response to 0 V to 4 V Step

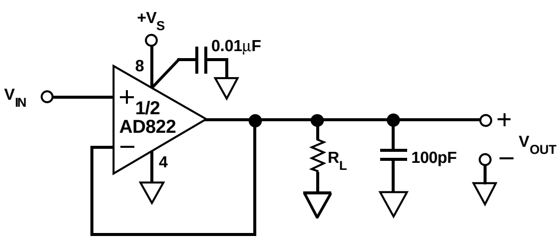

Figure 32. Unity Gain Follower

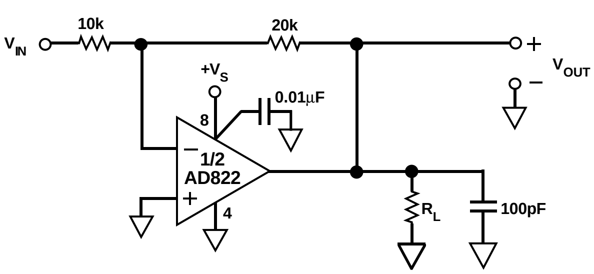

Figure 33. Gain of Two Inverter

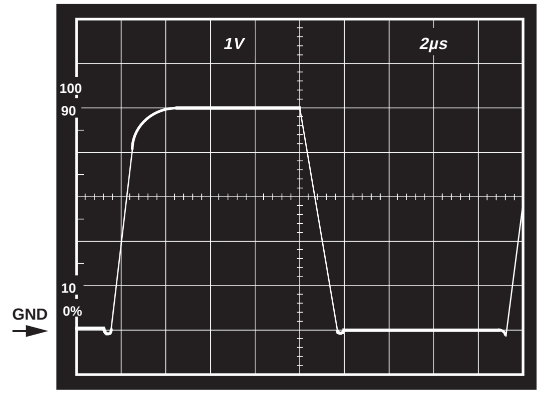

Figure 34. V_S = +5 V, 0 V; Unity Gain Follower Response to 0 V to 5 V Step

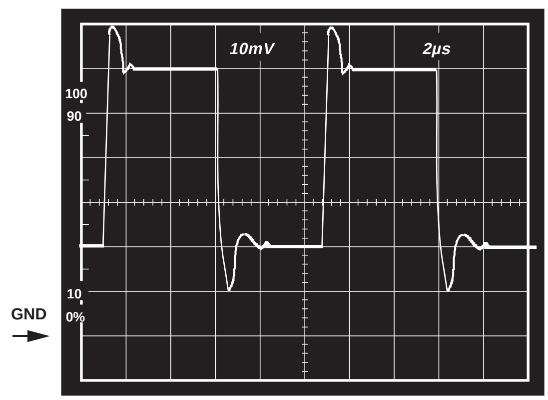

Figure 35. V_S = +5 V, 0 V; Unity Gain Follower Response, to 40 mV Step Centered 40 mV Above Ground, R_L = 10 kΩ

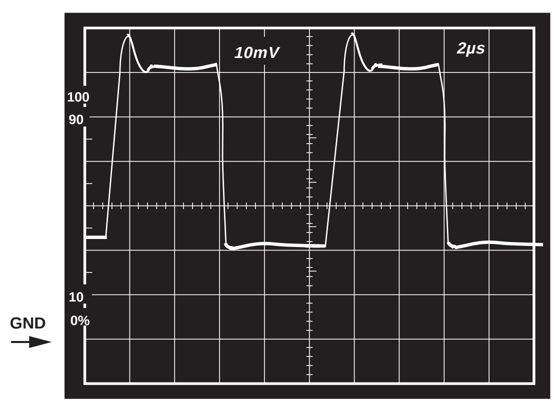

Figure 36. V_S = +5 V, 0 V; Gain of Two Inverter Response to 20 mV Step, Centered 20 mV Below Ground, R_L = 10 kΩ

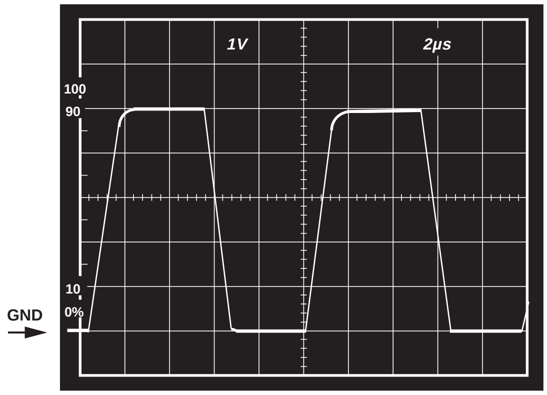

Figure 37. V_S = +5 V, 0 V; Gain of Two Inverter Response to 2.5 V Step Centered –1.25 V Below Ground, R_L = 10 kΩ

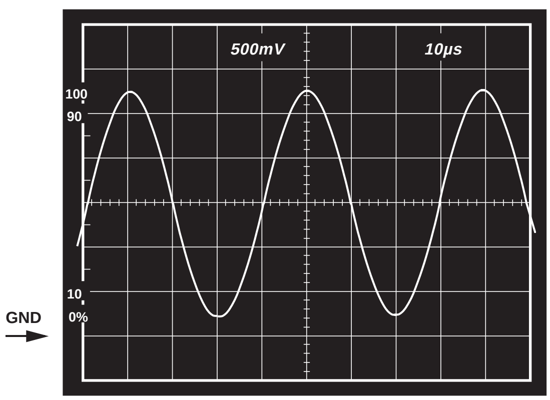

Figure 38. V_S = 3 V, 0 V; Gain of Two Inverter, V_{IN} = 1.25 V, 25 kHz, Sine Wave Centered at –0.75 V, R_L = 600 Ω

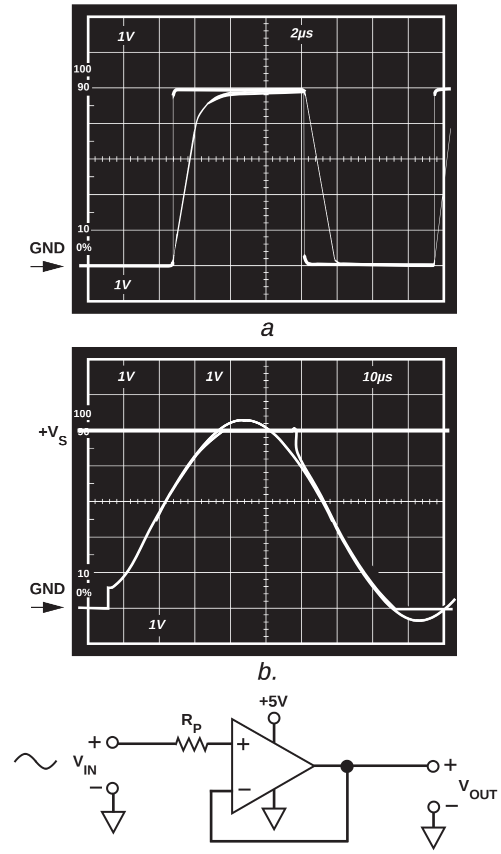

Figure 39. (a) Response with R_P = 0; V_{IN} from 0 to +V_S
(b) V_{IN} = 0 to +V_S + 200 mV
V_{OUT} = 0 to +V_S
R_P = 49.9 kΩ

APPLICATION NOTES

INPUT CHARACTERISTICS

In the AD822, n-channel JFETs are used to provide a low offset, low noise, high impedance input stage. Minimum input common-mode voltage extends from 0.2 V below $–V_S$ to 1 V less than $+V_S$. Driving the input voltage closer to the positive rail will cause a loss of amplifier bandwidth (as can be seen by comparing the large signal responses shown in Figures 31 and 34) and increased common-mode voltage error as illustrated in Figure 17.

The AD822 does not exhibit phase reversal for input voltages up to and including $+V_S$. Figure 39a shows the response of an AD822 voltage follower to a 0 V to +5 V ($+V_S$) square wave input. The input and output arc superimposed. The output tracks the input up to $+V_S$ without phase reversal. The reduced bandwidth above a 4 V input causes the rounding of the output wave form. For input voltages greater than $+V_S$, a resistor in series with the AD822's noninverting input will prevent phase reversal, at the expense of greater input voltage noise. This is illustrated in Figure 39b.

Since the input stage uses n-channel JFETs, input current during normal operation is negative; the current flows out from the input terminals. If the input voltage is driven more positive than $+V_S$ – 0.4 V, the input current will reverse direction as internal device junctions become forward biased. This is illustrated in Figure 4.

A current limiting resistor should be used in series with the input of the AD822 if there is a possibility of the input voltage exceeding the positive supply by more than 300 mV, or if an input voltage will be applied to the AD822 when $\pm V_S$ = 0. The amplifier will be damaged if left in that condition for more than 10 seconds. A 1 kΩ resistor allows the amplifier to withstand up to 10 volts of continuous overvoltage, and increases the input voltage noise by a negligible amount.

Input voltages less than $–V_S$ are a completely different story. The amplifier can safely withstand input voltages 20 volts below the minus supply voltage as long as the total voltage from the positive supply to the input terminal is less than 36 volts. In addition, the input stage typically maintains picoamp level input currents across that input voltage range.

The AD822 is designed for 13 nV/√Hz wideband input voltage noise and maintains low noise performance to low frequencies (refer to Figure 11). This noise performance, along with the AD822's low input current and current noise means that the AD822 contributes negligible noise for applications with source resistances greater than 10 kΩ and signal bandwidths greater than 1 kHz. This is illustrated in Figure 40.

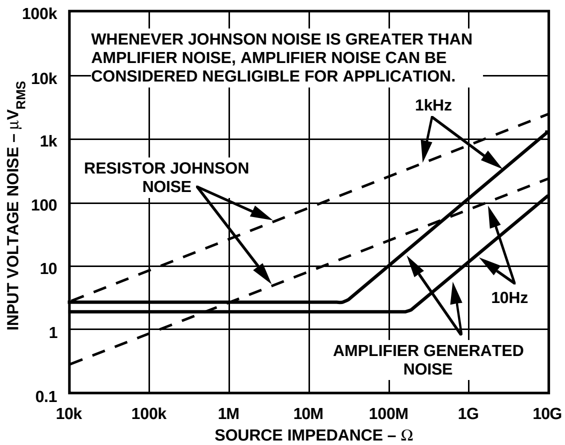

Figure 40. Total Noise vs. Source Impedance

OUTPUT CHARACTERISTICS

The AD822 s unique bipolar rail-to-rail output stage swings within 5 mV of the minus supply and 10 mV of the positive supply with no external resistive load. The AD822's approximate output saturation resistance is 40 Ω sourcing and 20 Ω sinking. This can be used to estimate output saturation voltage when driving heavier current loads. For instance, when sourcing 5 mA, the saturation voltage to the positive supply rail will be 200 mV, when sinking 5 mA, the saturation voltage to the minus rail will be 100 mV.

The amplifier's open-loop gain characteristic will change as a function of resistive load, as shown in Figures 7 through 10. For load resistances over 20 kΩ, the AD822's input error voltage is virtually unchanged until the output voltage is driven to 180 mV of either supply.

If the AD822's output is overdriven so as to saturate either of the output devices, the amplifier will recover within 2 μs of its input returning to the amplifier's linear operating region.

Direct capacitive loads will interact with the amplifier's effective output impedance to form an additional pole in the amplifier's feedback loop, which can cause excessive peaking on the pulse response or loss of stability. Worst case is when the amplifier is used as a unity gain follower. Figure 41 shows the AD822's pulse response as a unity gain follower driving 350 pF. This amount of overshoot indicates approximately 20 degrees of phase margin—the system is stable, but is nearing the edge. Configurations with less loop gain, and as a result less loop bandwidth, will be much less sensitive to capacitance load effects. Figure 42 is a plot of capacitive load that will result in a 20 degree phase margin versus noise gain for the AD822. Noise gain is the inverse of the feedback attenuation factor provided by the feedback network in use.

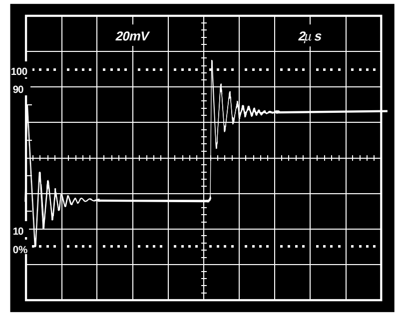

Figure 41. Small Signal Response of AD822 as Unity Gain Follower Driving 350 pF Capacitive Load

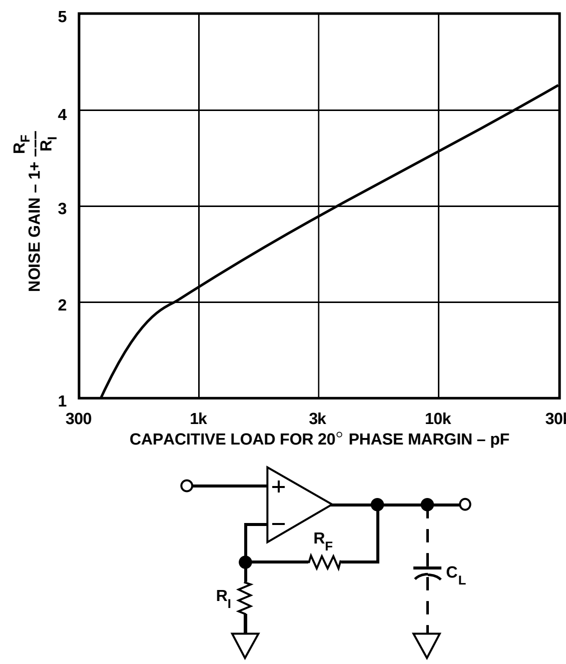

Figure 42. Capacitive Load Tolerance vs. Noise Gain

Figure 43 shows a method for extending capacitance load drive capability for a unity gain follower. With these component values, the circuit will drive 5,000 pF with a 10% overshoot.

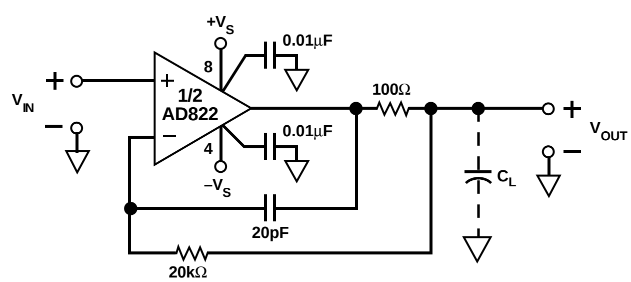

Figure 43. Extending Unity Gain Follower Capacitive Load Capability Beyond 350 pF

APPLICATIONS

Single Supply Voltage-to-Frequency Converter

The circuit shown in Figure 44 uses the AD822 to drive a low power timer, which produces a stable pulse of width t_1. The positive going output pulse is integrated by R1-C1 and used as one input to the AD822, which is connected as a differential integrator. The other input (nonloading) is the unknown voltage, V_{IN}. The AD822 output drives the timer trigger input, closing the overall feedback loop.

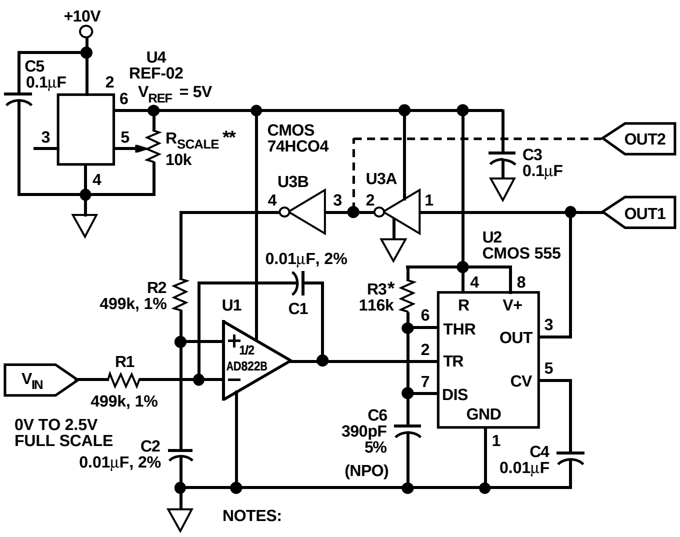

NOTES:

$f_{OUT} = V_{IN}/(VREF{*}t_1)$, $t_1 = 1.1{*}R3{*}C6$
= 25kHz f_S AS SHOWN.

* = 1% METAL FILM, <50ppm/°C TC

** = 10%, 20T FILM, <100ppm/°C TC

t_1 = 33µs FOR f_{OUT} = 20kHz @ V_{IN} = 2.0V

Figure 44. Single Supply Voltage-to-Frequency Converter

Typical AD822 bias currents of 2 pA allow megaohm-range source impedances with negligible dc errors. Linearity errors on the order of 0.01% full scale can be achieved with this circuit. This performance is obtained with a 5 volt single supply which delivers less than 1 mA to the entire circuit.

Single Supply Programmable Gain Instrumentation Amplifier

The AD822 can be configured as a single supply instrumentation amplifier that is able to operate from single supplies down to 3 V, or dual supplies up to ±15 V. Using only one AD822 rather than three separate op amps, this circuit is cost and power efficient. AD822 FET inputs' 2 pA bias currents minimize offset errors caused by high unbalanced source impedances.

An array of precision thin-film resistors sets the in amp gain to be either 10 or 100. These resistors are laser-trimmed to ratio match to 0.01%, and have a maximum differential TC of 5 ppm/°C.

Table I. AD822 In Amp Performance

Parameters	V_S = 3 V, 0 V	V_S = ±5 V
CMRR	74 dB	80 dB
Common-Mode Voltage Range	–0.2 V to +2 V	–5.2 V to +4 V
3 dB BW, G = 10	180 kHz	180 kHz
G = 100	18 kHz	18 kHz
$t_{SETTLING}$		
2 V Step (V_S = 0 V, 3 V)	2 µs	
5 V (V_S = ±5 V)		5 µs
Noise @ f = 1 kHz, G = 10	270 nV/√Hz	270 nV/√Hz
G = 100	2.2 µV/√Hz	2.2 µV/√Hz
I_{SUPPLY} (Total)	1.10 mA	1.15 mA

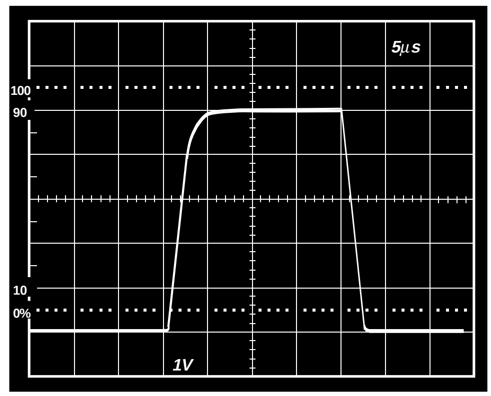

Figure 45a. Pulse Response of In Amp to a 500 mV p-p Input Signal; V_S = +5 V, 0 V; Gain = 10

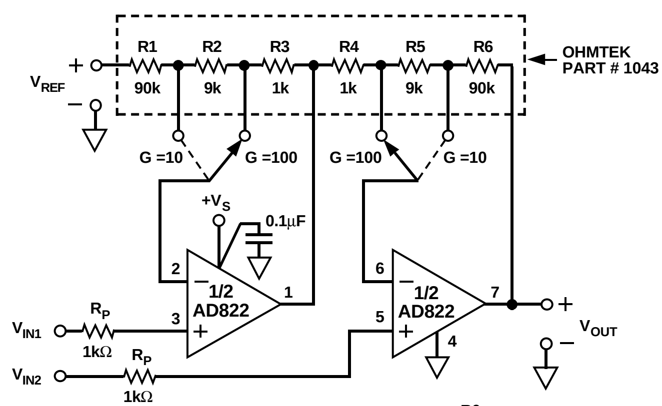

(G =10) $V_{OUT} = (V_{IN1} - V_{IN2})\left(1 + \frac{R6}{R4 + R5}\right) + V_{REF}$

(G =100) $V_{OUT} = (V_{IN1} - V_{IN2})\left(1 + \frac{R5 + R6}{R4}\right) + V_{REF}$

FOR R1 = R6, R2 = R5, AND R3 = R4

Figure 45b. A Single Supply Programmable Instrumentation Amplifier

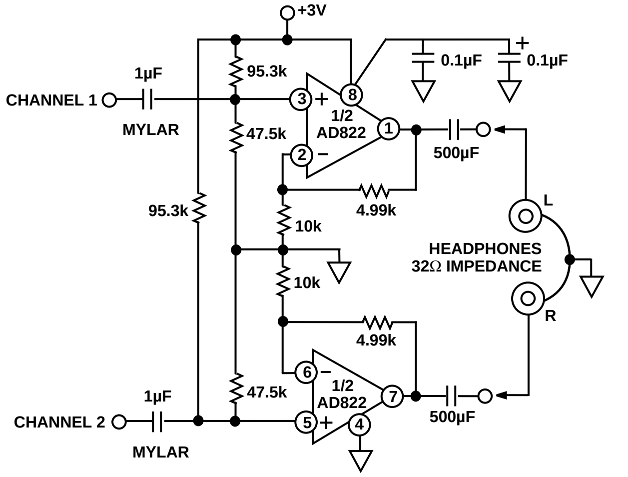

Figure 46. 3 Volt Single Supply Stereo Headphone Driver

3 Volt, Single Supply Stereo Headphone Driver

The AD822 exhibits good current drive and THD+N performance, even at 3 V single supplies. At 1 kHz, total harmonic distortion plus noise (THD+N) equals –62 dB (0.079%) for a 300 mV p-p output signal. This is comparable to other single supply op amps which consume more power and cannot run on 3 V power supplies.

In Figure 46, each channel s input signal is coupled via a 1 µF Mylar capacitor. Resistor dividers set the dc voltage at the noninverting inputs so that the output voltage is midway between the power supplies (+1.5 V). The gain is 1.5. Each half of the AD822 can then be used to drive a headphone channel. A 5 Hz high-pass filter is realized by the 500 µF capacitors and the headphones, which can be modeled as 32 ohm load resistors to ground. This ensures that all signals in the audio frequency range (20 Hz–20 kHz) are delivered to the headphones.

Low Dropout Bipolar Bridge Driver

The AD822 can be used for driving a 350 ohm Wheatstone bridge. Figure 47 shows one half of the AD822 being used to buffer the AD589—a 1.235 V low power reference. The output of +4.5 V can be used to drive an A/D converter front end. The other half of the AD822 is configured as a unity-gain inverter, and generates the other bridge input of –4.5 V. Resistors R1 and R2 provide a constant current for bridge excitation. The AD620 low power instrumentation amplifier is used to condition the differential output voltage of the bridge. The gain of the AD620 is programmed using an external resistor R_G, and determined by:

$$G = \frac{49.4\ k\Omega}{R_G} + 1$$

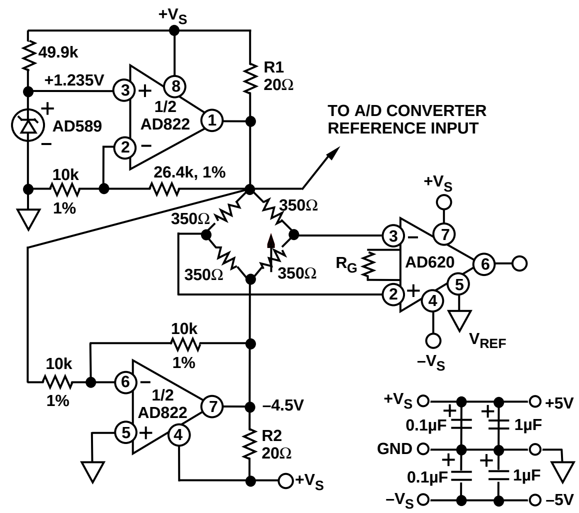

Figure 47. Low Dropout Bipolar Bridge Driver

C1821a–10–9/94

OUTLINE DIMENSIONS

Dimensions shown in inches and (mm).

Mini-DIP (N) Package

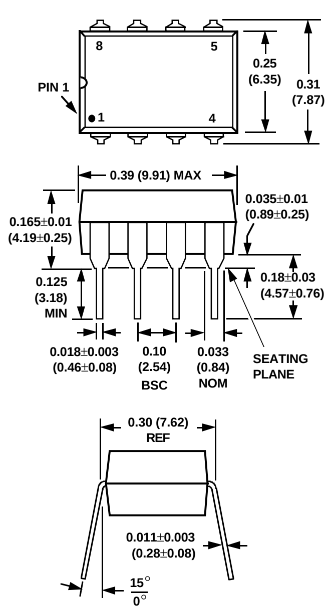

Cerdip (Q) Package

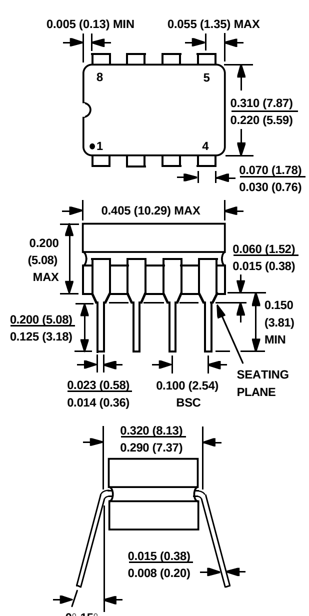

SOIC (R) Package

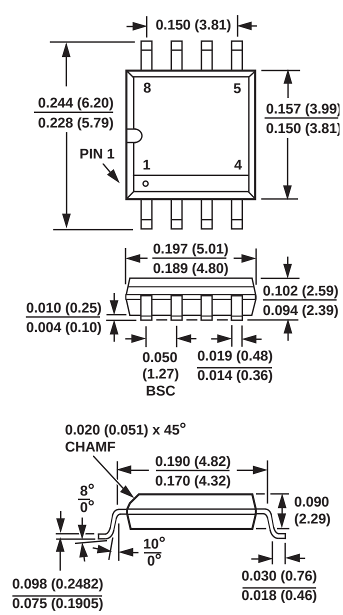

PRINTED IN U.S.A.